 doi:10.20944/preprints202004.0354.v1

Comparative analysis of machine learning algorithms for computer-assisted reporting based on fully automated cross-lingual RadLex® mappings

Máté E. Maros [1,2,*], MD, MSc; Chang Gyu Cho[1,2]; Andreas G. Junge[1], BSc; Benedikt Kämpgen[3], PhD; Victor Saase[1] MD, MSc, Fabian Siegel[2] MD, Frederik Trinkmann[2] MD, Thomas Ganslandt[2], PhD, MD; Holger Wenz[1], MD

[1]Department of Neuroradiology, Medical Faculty Mannheim, Heidelberg University, Mannheim, Germany.

[2]Department of Biomedical Informatics at the Heinrich-Lanz-Center, Medical Faculty Mannheim, Heidelberg University, Mannheim, Germany.

[3]Empolis Information Management GmbH, Kaiserslautern, Germany.

*Correspondence to:
Máté E. Maros, MD, MSc
Department of Neuroradiology,
Medical Faculty Mannheim, Heidelberg University, Mannheim, Germany
Theodor-Kutzer-Ufer 1-3,
68137 Mannheim, Germany
Tel: +49-621-383-2443, Fax: +49-621-383-2165,
E-mail: maros@uni-heidelberg.de
ORCID iD: 0000-0002-1589-8699

Keywords: machine learning, computer-assisted reporting (CAR), RadLex®, natural language processing (NLP), contextual reporting, The Alberta Stroke Programme Early CT Score (ASPECTS).

Tables: 3; Figures: 4.

Word count: 3951

 doi:10.20944/preprints202004.0354.v1

Highlights

- Cross-lingual RadLex® mapping-based machine learning can improve radiological report quality by context-sensitively suggesting key imaging biomarkers.
- Human expert-based key information extraction and fully automated RadLex®-based machine learning are comparable.
- By increasing key information content in reports, embedded assistive algorithms can substantially improve cohort selection for downstream analytics.
- The presented approach is robust and requires only a limited amount of expert labeled training data even for imbalanced classification tasks.
- We open-source our framework to facilitate research on developing task specific classifiers for computer-assisted reporting tools.

 doi:10.20944/preprints202004.0354.v1

Abstract

Objectives: Studies evaluating machine learning (ML) algorithms on cross-lingual RadLex® mappings for developing context-sensitive radiological reporting tools are lacking. Therefore, we investigated whether ML-based approaches can be utilized to assist radiologists in providing key imaging biomarkers – such as The Alberta stroke programme early CT score (APECTS).

Material and methods: A stratified random sample (age, gender, year) of CT reports (n=206) with suspected ischemic stroke was generated out of 3997 reports signed off between 2015-2019. Three independent, blinded readers assessed these reports and manually annotated clinico-radiologically relevant key features. The primary outcome was whether ASPECTS should have been provided (yes/no: 154/52). For all reports, both the findings and impressions underwent cross-lingual (German to English) RadLex®-mappings using natural language processing. Well-established ML-algorithms including classification trees, random forests, elastic net, support vector machines (SVMs) and boosted trees were evaluated in a 5 x 5-fold nested cross-validation framework. Further, a linear classifier (fastText) was directly fitted on the German reports. Ensemble learning was used to provide robust importance rankings of these ML-algorithms. Performance was evaluated using derivates of the confusion matrix and metrics of calibration including AUC, brier score and log loss as well as visually by calibration plots.

Results: On this imbalanced classification task SVMs showed the highest accuracies both on human-extracted- (87%) and fully automated RadLex® features (findings: 82.5%; impressions: 85.4%). FastText without pre-trained language model showed the highest accuracy (89.3%) and AUC (92%) on the impressions. Ensemble learner revealed that boosted trees, fastText and SVMs are the most important ML-classifiers. Boosted trees fitted on the findings showed the best overall calibration curve.

Conclusions: Contextual ML-based assistance suggesting ASPECTS while reporting neuroradiological emergencies is feasible, even if ML-models are restricted to be developed on limited and highly imbalanced data sets.

 doi:10.20944/preprints202004.0354.v1

Graphical abstract

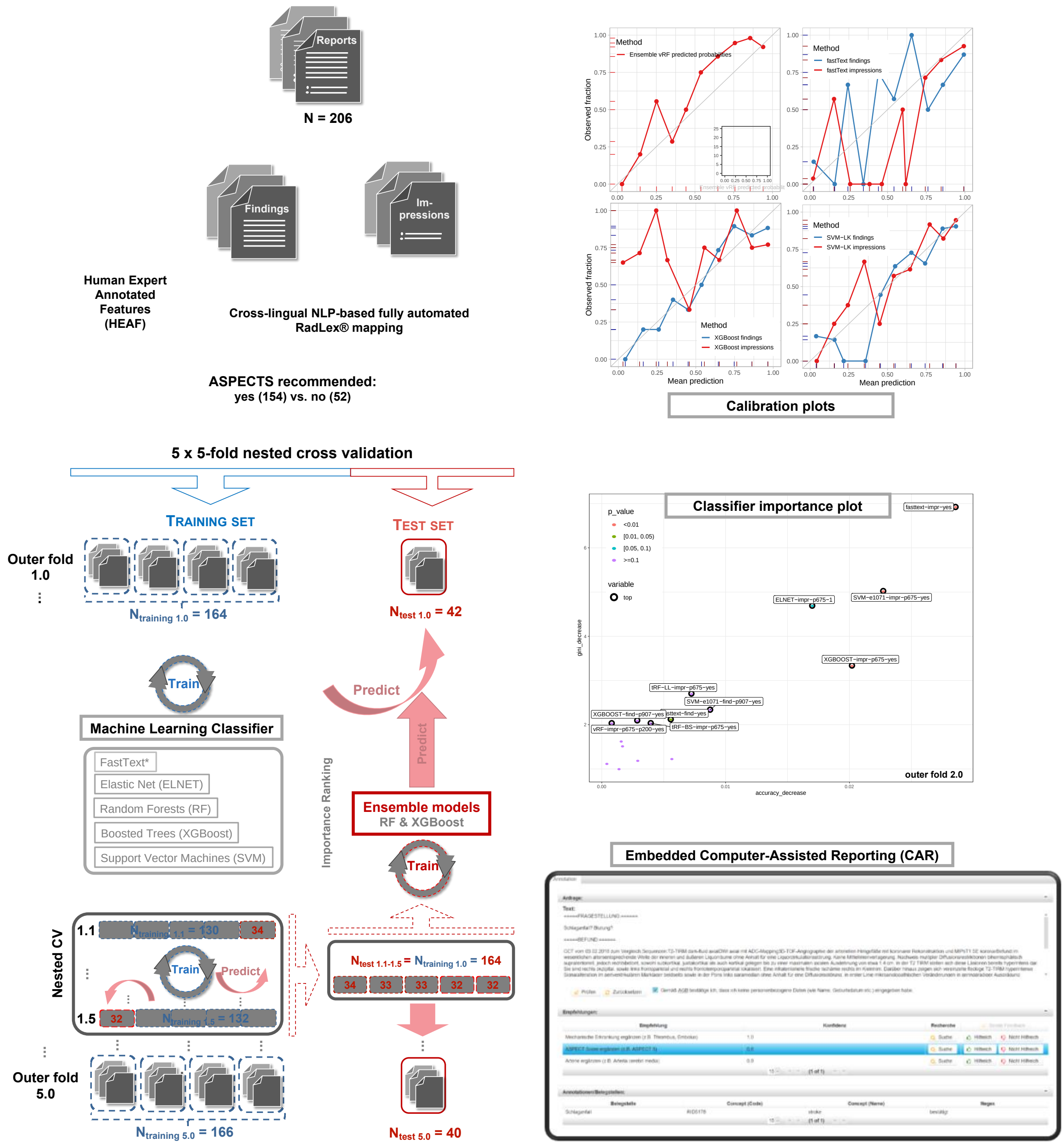

Preprints (www.preprints.org) | NOT PEER-REVIEWED | Posted: 19 April 2020 doi:10.20944/preprints202004.0354.v1

1. Introduction

There are no studies available that evaluate machine learning (ML) algorithms on cross-lingual RadLex® mappings to provide guidance when developing context-sensitive radiological reporting tools. Therefore, the purpose of our study was to compare the performance of ML algorithms developed on features extracted by human experts against those developed on fully automated cross-lingual RadLex® mappings of German radiological reports to English[1], in order to assist radiologists in providing key imaging biomarkers such as The Alberta Stroke Programme Early CT Score (APECTS)[2]. We show that this fully automated RadLex®-based approach is highly accurate even if the ML models were trained on limited and imbalanced expert labelled data sets[3-6]. Hence, this work provides a valuable blueprint for developing ML-based embedded applications for context-sensitive computer-assisted reporting (CAR) tools[7-10].

RadLex® is a comprehensive hierarchical lexicon of radiology terms that can be utilized in reporting, decision support and data mining[3]. RadLex® is freely available (v.4.0, http://radlex.org/) from the Radiological Society of North America (RSNA). It provides the foundation for further ontologies and procedural data bases such as the LOINC/RSNA Radiology Playbook[11] or Common Data Elements (CDE; RadElement; https://www.radelement.org/)[12]. The official translation of RadLex® to German by the German Society of Radiology (DRG) was made public in January 2018 and contained over 45,000 concepts.

ASPECTS is widely used in neurological emergencies to assess the extent of early ischemic changes on pretreatment non-contrast CT studies of the brain in patients with acute ischemic stroke of the anterior circulation[2]. It proved to be a robust and highly significant independent imaging biomarker to predict the outcome of intravenous thrombolysis, endovascular thrombectomy (EVT) and a surrogate for 90-day functional outcome [13]. Hence, ASPECTS serves as a key selection criterion for neurointerventional procedures. Accordingly, radiological textual metadata is of crucial importance when retrospectively selecting patient cohorts for clinical trials or extracting their imaging to develop computer vison algorithms[14-17]. Therefore, it is in the best interest of radiologists to report key radiological biomarkers like ASPECTS or other scoring systems such as the prostate (PI-RADS) or breast imaging-reporting data system (BI-RADS) to optimize downstream analytics and software

Preprints (www.preprints.org) | NOT PEER-REVIEWED | Posted: 19 April 2020 doi:10.20944/preprints202004.0354.v1

development using their data[18, 19]. Nonetheless, these key predictors are frequently missing from radiological reports as their overwhelming majority is still created as conventional narrative “free-text”[1, 20, 21].

ML methods have been introduced as powerful computer-aided diagnostic (CAD) tools[9, 15, 22] not only in image recognition and classification, but also in radiological reporting[23, 24]. Recently, complex deep transformer-based language models (TLM) are becoming the state-of-the-art (SOTA) in natural language processing (NLP)[25-29]. However, these models need considerable amount of general and domain specific corpora for training (even if using transfer learning approaches), which are scarce for languages other than English, particularly in the medical domain where creating expert-labelled high-quality training data is extremely resource intensive[30-33]. Despite achieving SOTA on certain classification tasks, TLMs represent black box methods and show susceptibility to subtle perturbances[31, 32]. Additionally, TLMs are seldom compared to baseline information retrieval methods such as shallow ML algorithms or linear classifiers (fastText) developed on bag-of-words (BOW)[34-36]. Therefore, we performed comprehensive analyses using an ensemble learning framework (Figure 1) that combined well-established ML algorithms as base classifiers including random forests (RF)[37], regularized logistic regression (ELNET)[38, 39], support vector machines (SVM)[40] and classification- (CART)[41] and boosted trees (XGBoost)[42] as well as fastText[36] on German computed tomography (CT) reports with suspected stroke and on their cross-lingual English RadLex® mappings using NLP[43].

As a proof of concept (“MyReportCheck”), we present a flexible open-source pipeline to swiftly develop robust ML classifiers for CAR tools in a language-agnostic fashion by using only limited expert labelled training data and cross-lingual bag-of-RadLex® mappings. We aimed to demonstrate the feasibility of our approach by automatically developing production-ready ASPECTS classifiers for CT stroke workups and compare it to methods developed on human expert annotations. Furthermore, we provide valuable guidance on choosing ML algorithms for similar context-sensitive recommendation tasks and make our data set available for the community to facilitate algorithm development and benchmarking.

 doi:10.20944/preprints202004.0354.v1

2. Materials and methods

2.1 Study cohort

The study was approved by the local ethics committee (approval nr.: 2017-825R-MA). Written informed consents were waived by the ethics committee due to the retrospective nature of the analyses. In this single-center retrospective cohort study, consecutive (German) radiological reports of cranial CTs with suspected ischemic stroke or hemorrhage between 01/2015-12/2019 were retrieved from local RIS (Syngo, Siemens, Healthineers, Erlangen, Germany) that contained the following key words in the clinical <request reason>, <request comment> or <request technical note> fields: “stroke”, “time window for thrombolysis”, “wake up”, “ischemia” and their (mis)spelling variations. A total of 4022 reports fulfilled the above criteria. After data cleaning, which excluded cases with missing requesting department, 3997 reports remained. Next, we generated a stratified random subsample (n=207, ~5.2%) based on age (binned into blocks of 10 years), sex (M|F), year (in which the imaging procedure was performed) and requesting department. During downstream analyses one report was removed because it contained only a reference to another procedure, leaving n=206 for later analyses (Figure 1). The extracted reports were all conventional free-texts and were signed off by senior radiologists with at least 4 years of experience in neuroradiology.

2.2 Information extraction by human experts

Three independent readers (R1, experience 3yrs; R2, 7yrs; R3, 10yrs) assessed the clinical questions, referring departments, findings and impressions of the reports. For each report, all readers independently evaluated whether ASPECTS was provided in the report or should have been provided in the report text (necessary: 154, 74.7%; not meaningful: 52, 25.3%]). Further, the two senior experts (R2 and R3) manually extracted clinico-radiologically relevant key features in the context of whether reporting ASPECTS is sensible based on the presence (yes | no) of ischemia (separately for new infarct demarcation and/or chronic post-ischemic defects);

bleeding (separately for each of the following entities: intracerebral hemorrhage (ICH), epi- (EDH), subdural hematoma (SDH), subarachnoid hemorrhage (SAH)); tumor; procedures including CT-angiography (CTA) or CT-perfusion (CTP); whether cerebral aneurysms or arteriovenous malformations (AVM) were detected; previous neurosurgical (clipping, tumor resection) or neurointerventional procedures (coiling); and previous imaging (within the last 1-3 days)[44, 45]. These human expert-annotated features (HEAF) were extracted concurrently from both the finding and impression sections and selected in accordance with national and international guidelines for diagnosing acute cerebrovascular diseases[44, 45]. HEAFs were used as input for ML algorithm development (Table 1). The feature matrix is available as supplementary data (heaf.csv) or GitHub download (https://github.com/mematt/ml4RadLexCAD/data).

2.3 RadLex® mapping pipeline

Both the findings and impression sections of each German report (n=206) were mapped to English RadLex® terms using a proprietary NLP tool, the Healthcare Analytics Services® (HAS) by Empolis Information Management GmbH (Kaiserslautern, Germany; https://www.empolis.com/en/). HAS implements a common NLP pipeline consisting of cleansing (e.g., replacement of abbreviations), contextualization (e.g. into segments "clinical information", "findings", and "conclusion"), concept recognition using RadLex®, and negation detection ("affirmed", "negated", and "speculated")[46]. For concept recognition, a full text index and morpho-syntactic operations such as tokenization, lemmatization, part of speech tagging, decompounding, noun phrase extraction and sentence detection were used. The full text index is an own implementation with features such as word/phrase search, spell check and ranking via similarity measures such as Levenshtein distance and BM25[47, 48]. The index is populated with synonyms for all RadLex® entities (both from the lexicon and by manual extensions), the morpho-syntactic operations are based on Rosette Base Linguistics (RBL) from

Basis Technology® (Cambridge, MA, USA; https://www.basistech.com/text-analytics/rosette/). For accuracy, RBL uses machine learning techniques such as perceptrons, support vector machines, and word embeddings. For negation detection, the NegEx algorithm was implemented in UIMA RUTA[46, 49]. No further pre-processing steps of the text were done.

Our RadLex® annotation and scoring pipeline (RASP), which utilizes the aforementioned API by Empolis, is available as a Shiny application at mmatt.shinyapps.io/rasp [35]. We used RASP to generate the document (i.e. report RadLex®) term matrix (DTM) of the complete data set over all reports (n=206) both for the findings and impression sections, respectively. In the DTM, each report is represented as a vector (i.e. bag-of-)RadLex® terms that occurred in the corpus[34, 35]. RadLex® terms were encoded in a binary fashion (0|1), whether the term was present or not. Further, each RadLex® term (i.e. feature) was annotated with three levels of confirmation or confidence "affirmed", "speculated", "negated", which was included in the feature name. This DTM provided the basis for fully automated RadLex®-based ML algorithm development (Table 2). The report-RadLex® term-matrices (i.e. DTMs) both for the findings and impression sections are available for direct download from our GitHub repository (https://github.com/mematt/ml4RadLexCAD/data) or as supplementary data (radlex-dtm-findings.csv and radlex-dtm-impressions.csv).

The performances of ML algorithms developed on these automated NLP-RadLex® mappings were then compared to those ML algorithms that were developed on the features extracted by human experts (HEAF). It is of note, however, that in its current iteration (v4.0) RadLex® does not contain certain key terms or concepts, one of which is ASPECTS. Although there is a CDE for ASPECTS classification (https://www.radelement.org/element/RDE173)[12]. Hence, extended IDs had to be created for such terms in the NLP annotation service, which are denoted as RadLex® ID Extended (RIDE), for example ASPECTS = RIDE172 in the DTMs.

2.4 Machine learning setup and classifier development

We performed extensive comparative analyses of well-established ML algorithms (base classifiers) to automatically learn rules required for ASPECTS reporting including single classification (and regression) trees (CART)[41], random forests (RF)[37], boosted decision trees (XGBoost)[42], elastic net-penalized binomial regression (ELNET)[38, 39] and support vector machines (SVM)[40]. Single CART was used to represent the baseline ML algorithm. A CART has the advantage that human readers can more easily interpret it, however its estimates are much less robust than ensembles of trees like RF[41, 50-52].

Each ML algorithm was fitted to the i) human expert-annotated features (HEAF; Table 1) and to the ii) RadLex® mapped DTMs both for the findings and impressions separately (Table 2). Because the effort of manually annotating the data set is large, especially if multiple experts annotate the same reports, we built upon our previously open-sourced protocol of a 5-fold nested cross-validation (CV) resampling scheme to have an objective and robust metric when comparing the performance of the investigated methods (Figure 1). Nested CV schemes allow for the proper training of secondary (e.g. calibrator or ensemble) models, without allowing for information leakage (Figure 1). To counter act the class imbalance (yes:no = 3:1) during CV-fold assignment (nfolds.RData), we performed stratified sampling. Also, RFs were downsampled to the minority class during training [53, 54].

In brief, the data set (n=206) was divided into stratified subsamples (outer fold training [$n_{outer.train}$=~164-166] – test set pairs [$n_{outer.test}$=40-42]) using 5-fold cross-validation (Figure 1; dashed blue and red boxes). Then, only the outer fold training sets were, yet again, subsampled using 5-fold CV, in order to create the nested/inner fold (training [$n_{inner.train}$=130-134] – test set pairs [$n_{inner.test}$=32-34]; Figure 1, nested CV). This was performed for both the findings and impressions sections using identical fold structures (Figure 1).

Hyperparameter tuning (i.e. training) of the investigated ML algorithms (base classifier) was performed within an extra-nested CV loop on the outer- or inner fold training sets. All models were fitted to the same data structure. Also, random seeds were fixed across all ML algorithms, in order to ensure direct comparability of their performance measures. ML algorithm training was optimized using either accuracy, brier score or log loss, which is indicated along the tuning parameter settings in Tables 2 & 3. For all ML algorithms probability outputs were also recorded and used to measure AUC and to create calibration plots. The average 5-fold CV model performances on the outer fold test sets are provided in Tables 1, 2 & 3.

Furthermore, we investigated whether a second layer ensemble model (based on all evaluated ML-base classifiers) could improve the overall performance. This second layer algorithm (either RF or XGBoost) was trained on the combined predictions (i.e. "ensemble") of the base ML models (i.e. CART, RF, XGBoost, ELNET, SVM and fastText) on the respective nested/innerfold test sets (Figure 1). Then, this tuned model was evaluated on the corresponding outer fold test set preventing any information leakage[6]. Additionally, the second layer "meta/ensemble" learner was used to derive importance rankings of the investigated ML base classifiers. For this, we have used mean decrease in accuracy without scaling when RF was used as the second layer "meta/ensemble" model, which has been suggested as the most robust setting when testing correlated features[6, 53, 55, 56]. Variable importance plots describing the RF meta-learner (Figure 3) were created using the randomForestExplainer package (v0.10.0.)[57]. Similarly, for importance ranking of boosted decision trees the gain metric was used[42]. Heretofore, we refer to second layer RF and XGBoost algorithms as meta/ensemble learners or models.

2.5 Text classification directly on German report texts using fastText

We used the open-source, lightweight fastText library (v0.9.1; https://fasttext.cc/) to learn linear text classifiers for ASPECTS recommendations on our data set[36] . The German report texts (both findings and impression sections) were preprocessed by excluding "([-.!?,'/()])". It is of note that fastText was only trained "on-the-fly" in each resampling loop on the corresponding subset of ~130-165 reports and we did not utilize any pre-trained word vector model for German[58]. This approach ensured a more direct comparability with the ML-classifiers developed on bag-of-RadLex® mappings. However, pre-trained word vector models for 157 languages, which were pre-trained on Common Crawl and Wikipedia by the fastText package authors are available for direct download (https://fasttext.cc/docs/en/crawl-vectors.html) [58]. We used the Python (v3.7) interface to fastText (https://github.com/facebookresearch/fastText/tree/master/python) on an Ubuntu 19.10 machine. FastText models were fitted both on the findings and impression sections respectively, using the same 5 x 5-fold nested-CV scheme as for the other ML algorithms with similar extra-nested CV loop for training on the outer- or inner fold training sets. Class label predictions and probability outputs were recorded and evaluated in the same manner as the investigated ML algorithms developed on HEAF and RadLex® mappings.

2.6 Statistical analyses

All statistical analyses were performed using the R language and environment for statistical programming (R v3.6.2, R Core Team 2019, Vienna Austria). The Cohen's kappa statistic was used to assess inter-rater agreement whether ASPECTS is recommended in a pairwise fashion for each of the two readers. To assess the overall agreement among the three readers, Fleiss' and Light's kappa was used.

Additionally, we created custom functions (https://github.com/mematt/ml4RadLexCAD/tree/master/calibration_plots) to visualize the probability outputs (i.e. calibration profiles) of the investigated ML-classifiers (Figure 3). Such calibration plots (or reliability diagrams) are useful graphical tools to visually assess the quality of calibration[59, 60]. Briefly, for real-life problems the true conditional probabilities are unknown, therefore the prediction space needs to be discretized into bins [60, 61]. A common approach is to use ten bins and assign cases to the corresponding bin where their predicted probabilities fall. For each bin the fraction of true positive cases (y-axis) is plotted against the mean of predicted classifier values (x-axis). Hence, an ideally calibrated classifier would lie on the diagonal line [59, 61]. P-values <0.05 were considered significant.

3. Results

3.1 Inter-rater reliability of human experts

Providing ASPECTS in the report would have been recommended by R1 in 156 (75.7%), by R2 in 154 (74.8%) and by R3 in 155/206 (75.2%) of the cases. The overall agreement between the three readers for "ASPECTS recommended" was $kappa_{Light}=0.747$ (n=206, z=4.6, $p=4.3\times10^{-6}$). The pairwise Cohen's kappa between R1 and R2 was 0.635 ($p<2\times10^{-16}$), which corresponded to 86.4% agreement. Between R1 and R3 it was 0.62 ($p<2\times10^{-16}$) corresponding to 85.9% agreement. Ratings of two (R2 and R3) experienced readers showed an almost perfect alignment kappa=0.987 ($p<2\times10^{-16}$) with 99.5% overall agreement.

3.2 Reliability between automated RadLex® mappings and expert-annotated labels

In this random subsample, which represents a robust cross-section of the daily praxis, ASPECTS was reported extremely rarely in 4/206 (1.9%). Three of which occurred both in the findings and impressions (3/4, 75%) section and one of which was only reported in the impression (1/4, 25%). The RASP tool correctly annotated all ASPECTS-negative (203/203) and ASPECTS-positive (3/3) finding sections. In the impressions, it misclassified one ASPECTS-positive (1/4, 25%) report as negative (1/206, 0.49%).

3.3 Performance of machine learning algorithms developed on human expert-annotated features (HEAF)

3.3.1 Single classification tree (CART)

CART demonstrated a 5-fold CV accuracy of 73.3% with the worst 63% AUC, BS (0.37) and LL (0.87) values among the tested ML-classifiers (Table 1).

3.3.2 Random forests (RF)

The default ("vanilla") RF classifier fitted on the 28 HEAF achieved a 5-fold CV accuracy of 81.5% with an AUC of 82% and corresponding BS and LL of 0.27 and 0.44, respectively (Table 1). Drastically reducing the feature space of vRF to only the nine (9/28: 32.1%) or five (5/28; 17.9%) most important predictors, had a comparably limited effect on the predictive performance of vRF: its accuracies decreased 12.8% and 7.7%, respectively; AUC decreased by ~16%; while BS (~37%) and LL (~27%) scores increased (Table 1).

Fine tuning the RF classifier using the BS (tRF_{BS}) and LL (tRF_{LL}) metrics slightly improved the overall accuracy without relevantly changing the calibration metrics of the vRF algorithm (Table 1). On the outer folds, both tRF_{BS} and tRF_{LL} limited the feature space similarly – to the 14 or 25-28 most important variables. Interestingly, ME-optimized RF (tRF_{ME}) achieved a slightly worse overall performance profile. Notably, on the outer fold 4.0, it limited the feature space to only the five RadLex® terms.

3.3.3 Elastic net-penalized binomial regression (ELNET)

ELNET showed a similar performance profile to RFs when fitted on the 28 HEAF but it achieved a narrower 5-fold CV confidence range of its accuracies (78-86%) while obtaining similar AUC, BS and LL scores (Table 1). The mixing parameter alpha (α) was chosen 3 out of 5 times to fit ridge (0) or ridge-like (0.1, 0.1) models while twice to fit lasso (1) or lasso-like (0.8) models on the outer folds.

3.3.4 Support vector machines (SVM)

On HEAF linear kernel SVMs (SVM-LK) achieved the highest 5-fold CV accuracy (87.4%) and lowest BS (0.22) and LL (0.37) scores while obtaining a similar AUC of ~80% to other ML classifiers (Table 1). The tuning parameter of C was selected as 1 on two outer folds suggesting a larger margin for the separating hyperplane while larger values of 10 or 100 were selected on the remaining three outer folds, suggesting a smaller-margin classifier.

3.3.5 Boosted decision trees (XGBoost)

Boosted decision trees were similarly accurate (80.6%) like tuned RF and ELNET. Despite the detailed tuning grid, XGBoost had overall somewhat worse performance profile than the other investigated ML algorithms, particularly AUC was lower at 70% for which we do not have a clear explanation.

3.4 Performance of machine learning algorithms developed on fully automated RadLex® mappings

3.4.1 Single classification tree (CART)

Directly applying a classification tree without optimizing its tree complexity (i.e. no pruning) showed on the findings similar overall accuracy (77.2%) to vRF with similar AUC and BS (Table 2) but with worse LL metrics. On the impressions, however, CART was tied for the 3rd best accuracy (85.0%) but still it showed low AUC (0.75) and high LL (0.58) values.

3.4.2 Random forests (RF)

Applying unsupervised variance filtering to select the top 33% most variable RadLex® mappings of the findings sections, improved the 5-fold CV accuracy of vRF by ~4.7%. In contrast, the same variance filtering on the impression sections did not relevantly (0.6%) improve vRF's accuracy (Table 2). Tuned RF models were slightly more accurate than the default vRF, however, tuning did not improve much upon the remaining calibration metrics.

3.4.3 Elastic net-penalized binomial regression (ELNET)

ELNET was the 3rd best-performing ML algorithm on the RadLex® features of the findings sections behind SVMs and XGBoost with similar BS and LL metrics but lower accuracy ($p_{Acc.vs.NIR}$ = 0.061) and AUC (Table 2). On the impression, it achieved the second highest 5-

fold CV accuracy (85.0%; 95%CI: 79.3-89.5%; $p_{Acc.vs.NIR}$ = 2.8×10-4) with corresponding second-best calibration profile (AUC: 86%; BS: 0.22; and LL: 037). On the outer folds of the impressions lasso or lasso-like settings (0.9-1) dominated the tuned α settings. ELNET had a better visual calibration profile on the impressions than on the findings (Figure 2A).

3.4.4 Support vector machines (SVM)

Linear kernel SVMs (SVM-LK) were the only classifiers that performed in the top 2 on the RadLex® feature spaces of both the findings ($p_{Acc.vs.NIR}$ = 5.1×10-3) and impressions ($p_{Acc.vs.NIR}$ = 1.4×10-4) sections (Table 2). SVM-LK had the highest AUC and lowest LL on the findings while on the impressions, it was overall the best-performing base ML-classifier. SVMs were comparably well-calibrated for both the findings and impressions, especially in the 0.5-1.0 probability domain (Figure 2B).

3.4.5 Boosted decision trees (XGBoost)

XGBoost performed particularly well on the RadLex® mappings of the findings – where the other ML algorithms (including fastText) struggled (Table 2). It showed the highest accuracy ($p_{Acc.vs.NIR}$ = 1.4×10-4) and lowest BS with corresponding slightly worse AUC and LL metrics (than the runner-up SVM-LK). Nevertheless, it had the best overall visual calibration profile on the reliability diagrams for the whole probability domain (Figure 2C). Compared to the findings, on the impressions XGBoost tuning implied a stronger subsampling of the features when constructing each tree, thereby strongly limiting the available predictor space. On the impressions, XGBoost performed similar to RF classifiers.

3.5. Linear models (fastText) fitted directly on German report text

When directly fitting the findings sections of the reports, the fastText algorithm showed a 5-fold CV accuracy of 83.0% (95%CI: 77.2-87.9%; $p_{Acc.vs.NIR}$ = 0.0030) with sensitivity of 94.8%, and specificity of 48.1% (PPV 84.4%, NPV: 75.8%), which corresponded to 84.4% precision and 89.3% F1 score. It achieved comparable AUC (81.1%) and BS (0.29) to other shallow ML-models trained on RadLex® mappings but showed markedly worse LL profile (0.98) suggesting "more certain" misclassifications.

FastText achieved the best results across all investigated ML algorithms fitted on the impressions sections of the reports. It showed a 5-fold CV accuracy of 89.3 % (95%CI: 84.3-93.2%; $p_{Acc.vs.NIR} = 1.35\times 10^{-7}$) with a balanced accuracy of 82.0%. Its predictive profile was in the 87-97% range (sensitivity: 96.8%; specificity: 67.3%; PPV 89.8%, NPV: 87.5%) with precision of 89.8% and F1 score of 93.1%. Furthermore, it showed the highest AUC (91.7%) with lowest BS (0.18) but yet again somewhat worse LL (0.55) than the RadLex®-based ML algorithms. FastText showed poor visual calibration profiles for both the findings and impressions in the lower probability domains (0-0.5), however it was almost ideally calibrated in the 0.75-1.0 domain of the impressions (Figure 2D).

3.6 Performance of the second layer meta/ensemble-learners

The second layer meta/ensemble RF learner, which was trained on predictions of the ML-classifiers of the findings sections, showed similar performance metrics (Table 3) as the top single ML-classifiers like SVM-LK, fastText and XGBoost (Table 2). Its accuracy was in the 77-88% 95%CI range ($p_{Acc.vs.NIR} = 1.8 \times 10^{-4}$) with 89.6% sensitivity; 65.3% specificity; 88.5% PPV; and 68% NPV which corresponded to a precision of 88.5% and F1 score of 89.6%. SVM-LK was chosen twice as the most important classifier while vRF, ELNET and XGBoost were each selected once on the five other folds (Figure 3A & D).

The 5-fold CV accuracy (89.3%) of the ensemble RF (Table 3), when using only the ML-models of the impressions as input features, was identical to the best predictor (fastText). But the 95% confidence interval got narrower and the LL score got considerably reduced (by 38%). This solely impressions-based ensemble achieved the following metrics: sensitivity 92.2%;

Preprints (www.preprints.org) | NOT PEER-REVIEWED | Posted: 19 April 2020 doi:10.20944/preprints202004.0354.v1

specificity 80.8%; PPV 93.4%, NPV 77.8% with corresponding precision of 93.4% and F1 score of 92.8%. FastText was chosen as the most important predictor for all outer fold test sets while as top 2_{nd} predictor XGBoost was chosen twice; ELNET, SVM-LK and tRF_{BS} were each selected once, respectively (Table 3; Figure 3B & E).

When the ML-classifier predictions of both the findings and impressions were the combined input for the second layer RF model, its accuracy, BS and LL slightly got worse (5-6%). The confusion matrix derivates were as follows: sensitivity 91.6%; specificity 80.8%; PPV 93.4%, NPV 76.4% with corresponding precision of 93.4% and F1 score of 92.5%. The variable importance rankings were dominated by ML-classifiers developed on the impression sections (Table 3; Figure 3C & F). The visual calibration profile of the RF ensemble developed on all ML-models (both findings and impressions; p =16) are presented in (Figure 2E & F).

On this same combined feature space (p=16), the second layer XGBoost ensemble showed a slightly reduced accuracy and worse calibration profiles than the RF ensemble (Table 3). Its predictive profile was in the 82-92% range ($p_{Acc.vs.NIR} = 6 \times 10_{-6}$; sensitivity: 93.5%; specificity: 69.2%; PPV 90.0%, NPV: 78.3%) with precision of 90% and F1 score of 91.7%. XGBoost selected fastText impressions 3x and SVM impressions 2x out of 5 on the outer folds as the most important variable based on the gain metric.

4. Discussion

In this work, we present a resource effective approach to develop production-ready embedded ML models for CAR tools, in order to assist radiologists in providing clinically relevant key biomarkers[9, 20, 62, 63]. To our knowledge, this is the first study that uses fully automated cross-lingual (German to English) RadLex® mappings-based machine learning to improve radiological reports by suggesting the key predictor ASPECTS in CT stroke workups. We demonstrated the feasibility of our automated RadLex® framework ("MyReportCheck", Figure 4) by comparing it to ML classifiers developed on human expert annotations. Furthermore, our ensemble learning setup provides objective rankings and a generalizable blueprint for choosing ML algorithms when developing classifiers for similar context-sensitive recommendation tasks[62, 64].

Although reporting templates have been developed to promote and standardize the best practice of radiological reporting[65-67], the majority of radiology reports are still created in free-text format[68, 69]. This limits the use of radiology reports in clinical research and algorithm development[63, 67, 69]. To overcome this, NLP pipelines including ML proved to be effective to annotate and to extract recommendations from reports[69, 70]. Nonetheless, studies dealing with ML algorithm development particularly for real-time context-sensitive assistance of radiologists while writing reports are scarce[64, 71]. Therefore, in this work, we focused on comprehensive and objective comparison of ML algorithms to provide technical guidance for developing these algorithms on limited (non-English) training data. For this, we have put an emphasis on the probabilistic evaluation and ranking of ML classifiers. This is less relevant for biomarker CAR recommendation systems but crucial for automated inference systems for scores such as BI-RADS[72] or PI-RADS[18].

We used a commercially available NLP pipeline that implements a common approach[8, 69] comprised of cleansing, contextualization and concept recognition as well as negation detection trained explicitly for German and English RadLex® mappings[1, 43]. This fully automated approach to generate bag-of-RadLex mappings is advantageous compared to standard BOW[35] approaches, as it already captures domain-specific knowledge including negation and affirmation[3]. Mikolov et al. proposed word2vec to create semantic word embeddings, which gained popularity in the field of radiology[5, 73]. However, word2vec struggles to properly handle out-of-vocabulary words[74, 75]. Thus, it needs to be combined with radiology domain-specific mappings. In contrast, our approach directly generates bag-of-RadLex terms for each report. We then combine all binary RadLex® term occurrences in our corpus (separately for findings and impressions) to generate the RadLex-DTMs. Therefore, our pipeline is also more robust for new or missing words e.g. if a new report does not contain certain terms (present in the training corpus), these can be easily substituted with 0 or new terms can be added to the DTM and the ML classifier can be swiftly retrained. This commercial NLP-based RadLex-mapping pipeline for creating DTMs is free for research purposes and can be easily utilized through our Shiny application.

Similar to previous studies[65, 69], we also flattened the hierarchical tree structure of RadLex® concepts and let the ML classifiers select subgroups of terms relevant to the classification task automatically during training. For a similar domain-specific semantic-dictionary mapping, as part of their hybrid word embedding model, Banerjee et al. created a custom ontology crawler that identified key terms for pulmonary embolism[76]. Another approach by Percha et al. included only partial flattening of RadLex®. They selected the eight most frequent parent categories that were used to learn word and RadLex® term vector representations for automatically expanding ontologies[5]. We have also found that certain key terms are missing from RadLex® and manually extended it. Other approaches to mitigate this problem and to increase interoperability, aim to combine multiple (both radiology-specific and general medical) ontologies or procedural databases such as RadLex®, LOINC/RSNA playbook, CDE from the RSNA and Systematized Nomenclature of Medicine Clinical Terms (SNOMED CT) as well as the International Classification of Diseases (v.10) Clinical Modification (ICD-10-CM)[74, 77-79].

All investigated ML algorithms were "CPU only" thereby imposing minimal hardware requirements and being quick both at train and test time[36]. These ML models have proven to be effective on both text classification[34, 36, 80] and other high-dimensional medical problems including high-throughput genomic microarray data[6, 81]. Additionally, we implemented a nested CV learning framework in order to objectively assess the importance of each ML base classifier and report section (i.e. findings and impressions) based on their probability estimates of recommending ASPECTS[6]. Zinov et al. also used a probabilistic ensemble learning setup to match lung nodule imaging features to text[71]. It is of note that there is multicollinearity both on the level of RadLex® mappings when training ML base classifiers and when combining the probability estimates of these ML classifiers on the second layer meta/ensemble-learner level. Default settings of RF (both in Python and R) are less robust for these scenarios due to the dilution of true features[6, 53, 55, 56]. To counter act dilution, we used the most robust metric of permutation-based importance (type=1) without scaling for all RF models. In contrast, boosted trees by design are less susceptible to correlation of features [42, 52]. The performance of the investigated ML algorithms is differently sensitive to the number of features[6, 81]. Based on results by limiting the feature space with unsupervised variance filtering, we suggest using all annotated RadLex® features as input and treating the number of features (p) as a tuning parameter during ML-algorithm training to achieve the best possible accuracies.

Preprints (www.preprints.org) | NOT PEER-REVIEWED | Posted: 19 April 2020 doi:10.20944/preprints202004.0354.v1

ML models developed on HEAF were similarly accurate (87%) to those developed on fully automated cross-lingual RadLex® mappings (~85%), although the latter models had substantially better calibration profiles (especially AUC and BS). This corresponded to results by Tan et al. on lumbar spine imaging when comparing rule-based methods to ML models[82]. On the more heterogeneous and larger RadLex® feature space of the findings sections, most ML models including fastText struggled but XGBoost performed best with an almost ideal calibration profile among all models (including those developed on the impressions). As impressions are expert-created condensed extracts of the most relevant information, ML performed substantially better (all > 80%). Accordingly, both RF and XGBoost meta/ensemble learners favored ML models that were developed on the impressions particularly fastText, SVM-LK and BS-tuned RF. These second layer meta/ensemble models achieved precision of 90-93%, recall: 92-94% and F1 score: 91-93%, which was well in line with the performance of information extraction model by Hassanpour et al. on a similarly sized (n=150) test set of multi-institutional chest CT reports[69].

The advantage of RadLex-based ML models compared to fastText is that they contain anatomical concepts and we can directly access negation information providing human interpretable explanation of the model. For fastText, such concepts are not necessarily learnable from limited training data or for more complex decision support scenarios other than ASPECTS. This was also supported by the fact that, despite being a baseline model, single CART performed remarkable well on the impressions implying that recommending ASPECTS is a less complex decision task.

The present study has certain limitations as it was a single-center, retrospective cross-sectional study of moderate size. Nonetheless, we selected a stratified random sample of ~200 reports from ~4000 reports from a period of 4 years, which robustly represented the general daily praxis. Our primary goal was to provide baseline performance metrics for well-established NLP and ML algorithms and linear classifiers with respect to radiology-specific biomarker (ASPECTS) recommendation tasks. Hence, there are natural extensions to our methodology including the switch to well-known neural network architectures both to generate RadLex® mappings[26, 83] and to create task-specific classifiers in an end-to-end manner such as convolutional (CNN)[24], recurrent neural networks (RNN)[72] or long short-term memory (LSTM) networks[63, 84]. However, fastText (with only a single hidden layer) has proven to be on a par with these more complex network architectures on several benchmarks[36]. Although, incorporating pre-trained language-specific word representations into fastText was expected to improve its accuracy we chose not to do so to allow for more direct performance comparisons with bag-of-RadLex-based ML classifiers[58].

Utilizing large transformer architectures[25, 27-29, 85] directly on German free-text reports would be a reasonable extension, however, sufficiently large non-English public radiology domain-specific corpora for transfer learning are lacking and the interpretability of TLMs is challenging[31]. Whether TLMs "truly learn" underlying concepts as a model of language or just extract spurious statistical correlations is a topic of active research[32, 33]. Thus, our CT stroke corpus can facilitate benchmarking of such models for the German radiological domain[31, 83, 85].

For recommending ASPECTS we used $p_{yes} > 0.5$ probability threshold. Optimizing this cutoff could further improve the performance metrics of the ML classifiers – for example by maximizing the Youden index[86].

To counteract class imbalance, we also explored upsampling, downsampling, random over-sampling and synthetic minority over-sampling techniques (SMOTE)[87], however, they did not improve the accuracy of ML classifiers on our data set (data not shown).

Regardless of these limitations, compared to text-based DL methods, our approach has some major advantages: i) building ML classifiers on top of cross-lingual RadLex® mappings incorporates domain-specific knowledge thereby only requiring a limited amount of expert

 doi:10.20944/preprints202004.0354.v1

labeled data – for which simple class labels are sufficient; ii) this approach can be easily adopted to any other language where RadLex® was translated by the local radiological society; iii) an ultimate benefit of our methodology is that it allows for the instant interoperability between languages especially the direct transportability of any ML model created for biomarker recommendation or inference from one language to another.

Preprints (www.preprints.org) | NOT PEER-REVIEWED | Posted: 19 April 2020 doi:10.20944/preprints202004.0354.v1

5. Conclusion

We showed that expert-based key information extraction and fully-automated RadLex mapping-based machine learning is comparable and requires only a limited amount of expert-labeled training data – even for highly imbalanced classification tasks. We performed detailed comparative analyses of well-established ML algorithms and identified those, which are best suited for automated rule learning on bag-of-RadLex® concepts (SVM, XGBoost and RF) and directly on German radiology report texts (fastText) through utilizing a nested CV learning framework.

Taken together, this work provides a generalizable probabilistic framework for developing embedded ML algorithms for CAR tools to context-sensitively suggest, not just ASPECTS but any required key biomarker information. Thereby improving report quality and facilitating cohort identification for downstream analyses.

 doi:10.20944/preprints202004.0354.v1

Data statement

Both the human expert annotated features (heaf.csv) and the fully automated NLP-based RadLex® mappings (term-report-matrices) are provided in our GitHub repository (https://github.com/mematt/ml4RadLexCAD/). The RadLex® annotation and scoring pipeline (RASP) is freely available for research purposes as Shiny application at www.mmatt.shinyapps.io/rasp . All tuned ML-model objects including the fold IDs for the 5 x 5-fold stratified nested CV scheme (nfolds.RData) are provided on GitHub. Additionally, we provide R code for ML-model training and for generating calibration plots presented in Fig. 3.

Acknowledgements

Funding: M.E.M., C.G.C. and B.K. gratefully acknowledge funding from the German Federal Ministry for Economic Affairs and Energy within the scope of Zentrales Innovationsprogramm Mittelstand (ZF 4514602TS8). M.E.M., C.G.C., F.S., F.T. and T.G. were supported by funding from the German Ministry for Education and Research (BMBF) within the framework of the Medical Informatics Initiative (MIRACUM Consortium: Medical Informatics for Research and Care in University Medicine; 01ZZ1801E).

Author contributions

M.E.M. conceptualized the study. A.G.J. and M.E.M. performed RIS data extraction and data preparation. M.E.M., C.G.C. and H.W. analyzed the reports and performed expert feature extraction. M.E.M. created the Shiny application. M.E.M. developed the machine learning framework. A.G.J. applied the linear language models. B.K. developed the connection to the RadLex® annotation service. F.S., F.T., V.S. and T.G. advised technical aspects of the study. H.W. and M.E.M. supervised the clinical aspects of the study. M.E.M, B.K. and H.W. wrote the manuscript. All authors critically reviewed the manuscript and approved the final version.

 doi:10.20944/preprints202004.0354.v1

Declaration/Conflict of interest

B.K. is an employee of Empolis Information Management GmbH. M.E.M., C.G.C. and B.K. received joint funding from the German Federal Ministry for Economic Affairs and Energy within the scope of Zentrales Innovationsprogramm Mittelstand. The founding sponsors had no role in the design of the study; in the collection, analyses, or interpretation of data; in the writing of the manuscript; and in the decision to publish the results. The other authors declare no conflicts of interest.

Preprints (www.preprints.org) | NOT PEER-REVIEWED | Posted: 19 April 2020 doi:10.20944/preprints202004.0354.v1

Table 1 | Summary table of performance measures of the investigated ML algorithms developed on human expert-annotated features (HEAF).

Report section	Method	ML Classifier	HEAF feature space	Rank	Software	Optimized metric	Tested hyperparameter space	Selected number of features or hyperparameter settings on outer fold 1.0-5.0	Accuracy# [min-max; %]	ME	AUC	BS	LL
Human Expert-Annotated Features (HEAF)	CART	CT	p=28 (all)		rpart [R]	ACC	rpart.control = default; cp = 0.01 no optimization (no pruning)	28	73.3 [66.7-79.2]	0.27	0.63	0.37	0.87
	vRF	RF	p=28 (all)	4	randomForest [R]	ME	ntree =500, mtry=5, p_{varsel} = 28	28	81.5 [73.8-92.7]	0.18	0.82	0.27	0.44
	vRF	RF	p=28 (all)		randomForest[R]	ME	ntree =500, mtry=5, p_{varsel} = 9	9	71.0 [59.5-82.9]	0.29	0.69	0.37	0.56
	vRF	RF	p=28 (all)		randomForest[R]	ME	ntree =500, mtry=5, p_{varsel} = 5	5	75.2 [68.3-83.3]	0.25	0.69	0.36	0.54
	tRF_{BS}	RF	p=28 (all)	2	randomForest[R]	BS	ntree = [100, 200, 300, … , 900, 1000]	28, 14, 14, 14, 14	83.1 [76.2-90.2]	0.17	0.81	0.27	0.44
	tRF_{ME}	RF	p=28 (all)		randomForest[R]	ME	mtry = [3, 4, 5, 6, 7]	28, 28, 14, 5, 14	79.6 [68.3-90.2]	0.20	0.79	0.29	0.46
	tRF_{LL}	RF	p=28 (all)	2	randomForest[R]	LL	p_{varsel} = [3, 5, 10, 14, 20, 25, 28]	25, 14, 14, 14, 14	83.1 [76.2-90.2]	0.17	0.81	0.27	0.44
	ELNET	ELNET	p=28 (all)	3	glmnet[R]	ME	α = [0, 0.1, 0.2, … , 0.8, 0.9, 1] λ = 10-fold CV with default hot-start	α = [0.1, 0.8, 0, 1, 0.1] λ = [0.195, 0.0688, 0.208, 0.0301, 0.1632]	82.0 [78.6-85.4]	0.18	0.79	0.27	0.43
	SVM-LK	SVM	p=28 (all)	1	e1071[R]	ME	C = [0.001, 0.01, 0.1, 1, 10, 100, 1000]	C = [1, 1, 100, 10, 10]	87.4 [82.9-90.2]	0.13	0.79	0.22	0.37
	XGBoost	BT	p=28 (all)	5	xgboost[R]	ME	nrouds/ntree = 100, max_depth = [3, 5, 6 ,8] eta = [0.1, 0.3] gamma = [0, 0.5, 1.0] colsample_bytree = [0.1, 0.25, 0.5, 0.693 (ln2)~$_{RF}$, 1]	nrouds = 100 max_depth = [5, 8, 5, 8, 3] eta = [0.1, 0.1, 0.1, 0.3, 0.1] gamma = [0, 0.5, 1, 0.5, 1] colsample_bytree = [1, 1, 0.5, 1, 0.5]	80.6 [75.0-85.7]	0.19	0.70	0.30	0.48

Accuracy#: the averaged 5-fold CV accuracy is calculated, ACC: accuracy, AUC: multiclass area under the ROC after Hand and Till (that can only be calculated if probabilities are scaled to 1), BS: Brier score, ME: misclassification error, LL: multiclass log loss, vRF and tRF: vanilla- and tuned random forests, ELNET: elastic net penalized multinomial logistic regression, SVM: support vector machines, LK: linear kernel SVM; XGBoost: extreme gradient boosting using trees as base learners, BT: boosted trees, CART: classification and regression trees; CT: classification tree; cp: complexity parameter used for CART node splitting (for this no optimization (pruning) was performed); ln(2)~$_{RF}$: column sampling (i.e. bootstrap) representing the settings equivalent to running RF in the xgboost library, [R]: R statistical software environment.

Preprints (www.preprints.org) | NOT PEER-REVIEWED | Posted: 19 April 2020 doi:10.20944/preprints202004.0354.v1

Table 2 | Summary table of performance measures of the investigated ML algorithms on the NLP-annotated bag-of-RadLex® features of the findings and impressions sections.

Report section	Method	ML Classifier	RadLex® feature space	Rank	Software	Optimized metric	Tested hyperparameter space	Selected number of features or hyperparameter settings on outer fold 1.0-5.0	Accuracy$^{\#}$ [min-max; %]	ME	AUC	BS	LL
Findings	CART	CT	p = 907	5	rpart [R]	ACC	rpart.control = default; cp = 0.01	p = 907	77.2 [70.8-82.7]	0.23	0.74	0.32	0.66
	vRF	RF	p=300 (us var.filt.)		randomForest [R]	ME	ntree =500, mtry=30, p_{varsel} = 200	p_{varsel} = 200	76.2 [71.4-85.4]	0.24	0.78	0.33	0.51
	vRF	RF	p=907 (all)		randomForest[R]	ME	ntree =500, mtry=30, p_{varsel} = 200	p_{varsel} = 200	72.8 [67.5-78.6]	0.27	0.78	0.33	0.50
	vRF	RF	p=907 (all)		randomForest[R]	ME	ntree =500, mtry=30, p_{varsel} = 20	p_{varsel} = 20	71.4 [62.5-75.6]	0.29	0.74	0.40	0.63
	tRF$_{BS}$	RF	p=907 (all)		randomForest[R]	BS	ntree = [200, 400, 600, … , 1400, 1600]	p_{varsel} = [500, 50, 100, 100, 50]	75.2 [71.4-81.0]	0.25	0.76	0.33	0.51
	tRF$_{ME}$	RF	p=907 (all)		randomForest[R]	ME	mtry = [20, 25, 30, 35, 40]	p_{varsel} = [907, 907, 907, 907, 907]	74.3 [67.5-83.3]	0.26	0.77	0.33	0.50
	tRF$_{LL}$	RF	p=907 (all)		randomForest[R]	LL	p_{varsel} = [10; 20; 50; 100; 200; 500; 907]	p_{varsel} = [50, 50, 50, 50, 50]	75.7 [70.7-85.7]	0.24	0.77	0.33	0.52
	ELNET	ELNET	p=907 (all)	4	glmnet[R]	ME	α = [0, 0.1, 0.2, …, 0.8, 0.9, 1] λ = 10-fold CV with default hot-start	α = [0.2, 0.7, 0.9, 1, 0.1] λ = [0.2685, 0.134, 0.0793, 0.114, 0.397]	79.6 [76.2-82.9]	0.20	0.75	0.29	0.46
	SVM-LK	SVM	p=907 (all)	3	e1071[R]	ME	C = [0.001, 0.01, 0.1, 1, 10]	C = [0.1, 0.1, 0.1, 0.1, 0.1]	82.5 [78.6-85.4]	0.18	0.80	0.27	0.43
	XGBoost	BT	p=907 (all)	1	xgboost[R]	ME	nrouds/ntree = 100, max_depth = [3, 5, 6 ,8] eta = [0.1, 0.3] gamma = [0, 0.5, 1.0] colsample_bytree = [0.1, 0.25, 0.5, 0.693 (ln2)$\sim_{RF}$, 1]	nrouds = 100 max_depth = [5, 8, 5, 8, 3] eta = [0.1, 0.1, 0.1, 0.3, 0.1] gamma = [0, 0.5, 1, 0.5, 1] colsample_bytree = [1, 1, 0.5, 1, 0.5]	85.4 [80.9-90.2]	0.15	0.78	0.25	0.45
	fastText	linear	direct fit on text	2	Fasttext [Python]	ACC & LL	default	-	83.0 [81.0-85.4]	0.17	0.81	0.29	0.98
Impressions	CART	CT	p=675	4	rpart [R]	ACC	rpart.control = default; cp = 0.01	p=675	85.0 [79.3-89.5]	0.15	0.75	0.26	0.58
	vRF	RF	p=300 (us var.filt.)		randomForest [R]	ME	ntree =500, mtry=26, p_{varsel} = 200	p_{varsel} = 200	83.0 [71.4-88.1]	0.17	0.87	0.25	0.39
	vRF	RF	p=675 (all)		randomForest [R]	ME	ntree =500, mtry=26, p_{varsel} = 200	p_{varsel} = 200	82.5 [71.4-88.1]	0.17	0.87	0.25	0.39
	vRF	RF	p=675 (all)		randomForest [R]	ME	ntree =500, mtry=26, p_{varsel} = 20	p_{varsel} = 20	78.2 [70-85.4]	0.22	0.81	0.30	0.49
	tRF$_{BS}$	RF			randomForest [R]	BS		p_{varsel} = [200, 100, 200, 500, 200]	80.0 [69.0-87.8]	0.20	0.85	0.26	0.41
	tRF$_{ME}$	RF	p=675 (all)		randomForest [R]	ME	ntree = [200, 400, 600, …, 1400, 1600] mtry = [21, 26, 31, 36, 41] p_{varsel} = [10; 20; 50; 100; 200; 500; 675] nodesize = [1; 2 (1%); 10 (5%)]	p_{varsel} = [200, 675, 200, 675, 500]	83.0 [69.0-90.5]	0.17	0.85	0.25	0.41
	tRF$_{LL}$	RF			randomForest [R]	LL		p_{varsel} = [50, 100, 50, 500, 50]	79.6 [71.4-87.8]	0.20	0.84	0.27	0.42
	ELNET	ELNET	p=675 (all)	3	Glmnet [R]	ME	α = [0, 0.1, 0.2, …, 0.8, 0.9, 1] λ = 10-fold CV with default hot-start	α = [0.9, 0.4, 1, 0, 0.9] λ = [0.056-2.01]	85.0 [82.9-88.1]	0.15	0.85	0.22	0.37
	SVM-LK	SVM	p=675 (all)	2	e1071 [R]	ME	C = [0.001, 0.01, 0.1, 1, 10]	C = [0.1, 0.1, 0.01, 0.1, 0.01]	85.4 [80.0-90.2]	0.15	0.86	0.21	0.36
	XGBoost	BT	p=675 (all)	5	xgboost [R]	ME	nrouds/ntree = 100, max_depth = [3, 5, 6 ,8] eta = [0.1, 0.3] gamma = [0, 0.5, 1.0] colsample_bytree = [0.1, 0.25, 0.5, 0.693 (ln2)$\sim_{RF}$, 1.0]	nrouds = 100 max_depth = [5, 3, 6, 5, 6] eta = [0.3, 0.3, 0.1, 0.1, 0.3] gamma = [0, 0, 1, 0.5, 0.5] colsample_bytree = [0.1, 0.25, 0.1, 1, 0.1]	83.0 [71.4-90.2]	0.17	0.83	0.26	0.44
	fastText	linear	direct fit on text	1	Fasttext [Py]	ACC & LL	default	-	89.3 [83.3-97.6]	0.11	0.92	0.18	0.55

Accuracy#: the averaged 5-fold CV accuracy is calculated, ACC: accuracy, AUC: multiclass area under the ROC after Hand and Till (that can only be calculated if probabilities are scaled to 1), us var.filt: unsupervised variance filtering using p=300 most variable RadLex® terms -this step was previous of training to prevent information leakage, BS: Brier score, ME: misclassification error, LL: multiclass log loss, vRF and tRF: vanilla- and tuned random forests, ELNET: elastic net penalized multinomial logistic regression, SVM: support vector machines, LK: linear kernel SVM; XGBoost: extreme gradient boosting using trees as base learners, BT: boosted trees, CART: classification and regression trees; CT: classification tree; cp: complexity parameter used for CART node splitting (for this no optimization (pruning) was performed); ln(2)$\sim_{RF}$: column sampling (i.e. bootstrap) representing the settings equivalent to running RF in the xgboost library, [R]: R statistical software environment; [Py] Python v3.7 programming language.

Preprints (www.preprints.org) | NOT PEER-REVIEWED | Posted: 19 April 2020 doi:10.20944/preprints202004.0354.v1

Table 3 | Summary table of performance measures of the second layer meta/ensemble learners (random forests and boosted trees) combining the predictions of all RadLex®-based ML base classifiers from the findings and impression sections.

Ensemble ML-algorithm	Classifiers	Number of features (ML-model outputs)	Most important ML-classifiers / outer fold	Optimized metric	Hyperparameters	Selected number of features or hyperparameter settings on outer fold 1.0-5.0	Accuracy$^{\#}$ [95%CI]	ME	AUC	BS	LL
vRF	vRF tRF_{BS}, tRF_{ME}, tRF_{LL}, ELNET, SVM-LK, XGBoost, fastText	8x ML-models (findings)	Top 1: vRF-find 1/5 SVM-find 2/5 ELNET-find 1/5 XGBoost 1/5 Top 2: XGBoost-find 1/5 tRF-ME-find 2/5 fasstext-find 1/5 ELNET-find 1/5	ME	ntree =500, mtry=2, p_{varsel} = 8	p_{varsel} = 8	83.5 [77.7-88.3]	0.17	0.83	0.29	0.47
vRF	vRF tRF_{BS}, tRF_{ME}, tRF_{LL}, ELNET, SVM-LK, XGBoost, fastText	8x ML-models (impressions)	Top 1: fasstext-impr 5/5 Top 2: svm-impr 1/5 XGBoost-impr 2/5 tRF-BS-impr 1/5 ELNET-impr 1/5	ME	ntree =500, mtry=2, p_{varsel} = 8	p_{varsel} = 8	89.3 [84.3-93.2]	0.11	0.90	0.19	0.34
vRF	vRF tRF_{BS}, tRF_{ME}, tRF_{LL}, ELNET, SVM-LK, XGBoost, fastText	16x ML-models (8x findings & 8x impressions)	Top 1: fasstext-impr 5/5 Top 2: svm-impr 3/5 tRF-BS-impr 1/5 ELNET-impr 1/5	ME	ntree =500, mtry=4, p_{varsel} = 16	p_{varsel} = 16	88.8 [83.7-92.8]	0.11	0.90	0.20	0.36
XGBoost	vRF tRF_{BS}, tRF_{ME}, tRF_{LL}, ELNET, SVM-LK, XGBoost, fastText	16x ML-models (findings & impressions)	Top 1: fasstext-impr 3/5 svm-impr 2/5 Top 2: fasstext-impr 2/5 tRF-BS-impr 2/5 svm-impr 1/5	ME	nrouds/ntree = [5, 10, 25, 50, 75, 100] max_depth = [3, 5, 6 ,8] eta = [0.01, 0.1, 0.3] gamma = [0, 0.001, 0.01, 0.1, 0.5, 1] colsample_bytree = [0.1, 0.25, 0.5, 0.693 $(ln2)_{\sim RF}$, 1.0], min_child_weight = 1, subsample = 1	nrounds = [75, 5, 75, 5, 10] max_depth = [3, 6, 5, 3, 5] eta = [0.3, 0.01, 0.1, 0.01, 0.1] gamma = [1, 0.01, 0.1, 0, 0.5] colsample_bytree = [0.1, 0.5, $ln2_{\sim RF}$, 0.1, 0.25]	87.4 [82.0-91.6]	0.13	0.87	0.30	0.46

AUC: multiclass area under the ROC after Hand and Till (that can only be calculated if probabilities are scaled to 1), us var.filt: unsupervised variance filtering using p=300 most variable RadLex® terms -this step was previous of training to prevent information leakage, BS: Brier score, ME: misclassification error, LL: multiclass log loss, vRF and tRF: vanilla- and tuned random forests, ELNET: elastic net penalized multinomial logistic regression, SVM: support vector machines, LK: linear kernel SVM, n.SV: number of support vectors; XGBoost: extreme gradient boosting using trees as base learners, BT: boosted trees.

 doi:10.20944/preprints202004.0354.v1

References:

[1] F. Jungmann, B. Kämpgen, P. Mildenberger, I. Tsaur, T. Jorg, C. Düber, P. Mildenberger, R. Kloeckner, Towards data-driven medical imaging using natural language processing in patients with suspected urolithiasis, International Journal of Medical Informatics (2020) 104106.
[2] P.A. Barber, A.M. Demchuk, J. Zhang, A.M. Buchan, Validity and reliability of a quantitative computed tomography score in predicting outcome of hyperacute stroke before thrombolytic therapy. ASPECTS Study Group. Alberta Stroke Programme Early CT Score, Lancet 355(9216) (2000) 1670-4.
[3] C.P. Langlotz, RadLex: a new method for indexing online educational materials, Radiographics : a review publication of the Radiological Society of North America, Inc 26(6) (2006) 1595-7.
[4] R.S.o.N. America, RadLex radiology lexicon. http://www.radlex.org/. (Accessed 11.11.2019 2019).
[5] B. Percha, Y. Zhang, S. Bozkurt, D. Rubin, R.B. Altman, C.P. Langlotz, Expanding a radiology lexicon using contextual patterns in radiology reports, Journal of the American Medical Informatics Association : JAMIA 25(6) (2018) 679-685.
[6] M.E. Maros, D. Capper, D.T.W. Jones, V. Hovestadt, A. von Deimling, S.M. Pfister, A. Benner, M. Zucknick, M. Sill, Machine learning workflows to estimate class probabilities for precision cancer diagnostics on DNA methylation microarray data, Nature Protocols 15(2) (2020) 479-512.
[7] M.D. Mamlouk, P.C. Chang, R.R. Saket, Contextual Radiology Reporting: A New Approach to Neuroradiology Structured Templates, AJNR Am J Neuroradiol 39(8) (2018) 1406-1414.
[8] E. Pons, L.M. Braun, M.G. Hunink, J.A. Kors, Natural Language Processing in Radiology: A Systematic Review, Radiology 279(2) (2016) 329-43.
[9] E.J. Topol, High-performance medicine: the convergence of human and artificial intelligence, Nature Medicine 25(1) (2019) 44-56.
[10] J.J. Titano, M. Badgeley, J. Schefflein, M. Pain, A. Su, M. Cai, N. Swinburne, J. Zech, J. Kim, J. Bederson, J. Mocco, B. Drayer, J. Lehar, S. Cho, A. Costa, E.K. Oermann, Automated deep-neural-network surveillance of cranial images for acute neurologic events, Nature Medicine 24(9) (2018) 1337-1341.
[11] D.J. Vreeman, S. Abhyankar, K.C. Wang, C. Carr, B. Collins, D.L. Rubin, C.P. Langlotz, The LOINC RSNA radiology playbook - a unified terminology for radiology procedures, Journal of the American Medical Informatics Association : JAMIA 25(7) (2018) 885-893.
[12] D.L. Rubin, C.E. Kahn, Jr., Common Data Elements in Radiology, Radiology 283(3) (2017) 837-844.
[13] M. Goyal, B.K. Menon, W.H. van Zwam, D.W. Dippel, P.J. Mitchell, A.M. Demchuk, A. Davalos, C.B. Majoie, A. van der Lugt, M.A. de Miquel, G.A. Donnan, Y.B. Roos, A. Bonafe, R. Jahan, H.C. Diener, L.A. van den Berg, E.I. Levy, O.A. Berkhemer, V.M. Pereira, J. Rempel, M. Millan, S.M. Davis, D. Roy, J. Thornton, L.S. Roman, M. Ribo, D. Beumer, B. Stouch, S. Brown, B.C. Campbell, R.J. van Oostenbrugge, J.L. Saver, M.D. Hill, T.G. Jovin, Endovascular thrombectomy after large-vessel ischaemic stroke: a meta-analysis of individual patient data from five randomised trials, Lancet 387(10029) (2016) 1723-31.
[14] A. Gerstmair, P. Daumke, K. Simon, M. Langer, E. Kotter, Intelligent image retrieval based on radiology reports, European radiology 22(12) (2012) 2750-2758.
[15] D. Pinto Dos Santos, B. Baessler, Big data, artificial intelligence, and structured reporting, European radiology experimental 2(1) (2018) 42.
[16] A. Rajkomar, E. Oren, K. Chen, A.M. Dai, N. Hajaj, M. Hardt, P.J. Liu, X. Liu, J. Marcus, M. Sun, Scalable and accurate deep learning with electronic health records, NPJ Digital Medicine 1(1) (2018) 18.
[17] A. Rajkomar, J. Dean, I. Kohane, Machine Learning in Medicine, New England Journal of Medicine 380(14) (2019) 1347-1358.
[18] N. Westhoff, F. Siegel, C. Peter, S. Hetjens, S. Porubsky, T. Martini, J. von Hardenberg, M.S. Michel, J. Budjan, M. Ritter, Defining the target prior to prostate fusion biopsy: the effect of MRI reporting on cancer detection, World journal of urology 37(2) (2019) 327-335.
[19] E.S. Burnside, E.A. Sickles, L.W. Bassett, D.L. Rubin, C.H. Lee, D.M. Ikeda, E.B. Mendelson, P.A. Wilcox, P.F. Butler, C.J. D'Orsi, The ACR BI-RADS experience: learning from history, J Am Coll Radiol 6(12) (2009) 851-60.
[20] Y. Hong, C.E. Kahn, Jr., Content analysis of reporting templates and free-text radiology reports, J Digit Imaging 26(5) (2013) 843-9.
[21] C.E. Kahn Jr, C.P. Langlotz, E.S. Burnside, J.A. Carrino, D.S. Channin, D.M. Hovsepian, D.L. Rubin, Toward best practices in radiology reporting, Radiology 252(3) (2009) 852-856.
[22] G. Choy, O. Khalilzadeh, M. Michalski, S. Do, A.E. Samir, O.S. Pianykh, J.R. Geis, P.V. Pandharipande, J.A. Brink, K.J. Dreyer, Current Applications and Future Impact of Machine Learning in Radiology, Radiology 288(2) (2018) 318-328.
[23] R.C. Mayo, J. Leung, Artificial intelligence and deep learning - Radiology's next frontier?, Clinical imaging 49 (2018) 87-88.
[24] M.C. Chen, R.L. Ball, L. Yang, N. Moradzadeh, B.E. Chapman, D.B. Larson, C.P. Langlotz, T.J. Amrhein, M.P. Lungren, Deep Learning to Classify Radiology Free-Text Reports, Radiology 286(3) (2018) 845-852.
[25] J. Devlin, M.-W. Chang, K. Lee, K. Toutanova, Bert: Pre-training of deep bidirectional transformers for language understanding, arXiv preprint arXiv:1810.04805 (2018).
[26] M.E. Peters, M. Neumann, M. Iyyer, M. Gardner, C. Clark, K. Lee, L. Zettlemoyer, Deep contextualized word representations, arXiv preprint arXiv:1802.05365 (2018).
[27] A. Radford, K. Narasimhan, T. Salimans, I. Sutskever, Improving language understanding by generative pre-training, URL https://s3-us-west-2. amazonaws. com/openai-assets/researchcovers/languageunsupervised/language understanding paper. pdf (2018).
[28] V. Sanh, L. Debut, J. Chaumond, T. Wolf, DistilBERT, a distilled version of BERT: smaller, faster, cheaper and lighter, arXiv preprint arXiv:1910.01108 (2019).

[29] M. Shoeybi, M. Patwary, R. Puri, P. LeGresley, J. Casper, B. Catanzaro, Megatron-lm: Training multi-billion parameter language models using gpu model parallelism, arXiv preprint arXiv:1909.08053 (2019).
[30] P. Richter-Pechanski, S. Riezler, C. Dieterich, De-Identification of German Medical Admission Notes, GMDS, 2018, pp. 165-169.
[31] B. Heinzerling, NLP's Clever Hans Moment has Arrived, 2019. https://thegradient.pub/nlps-clever-hans-moment-has-arrived/. (Accessed August 26, 2019 2019).
[32] T. Niven, H.-Y. Kao, Probing neural network comprehension of natural language arguments, arXiv preprint arXiv:1907.07355 (2019).
[33] C. Wang, M. Li, A.J. Smola, Language models with transformers, arXiv preprint arXiv:1904.09408 (2019).
[34] C.D. Manning, P. Raghavan, H. Schütze, Introduction to information retrieval, Cambridge university press Cambridge2008.
[35] M.E. Maros, R. Wenz, A. Forster, M.F. Froelich, C. Groden, W.H. Sommer, S.O. Schonberg, T. Henzler, H. Wenz, Objective Comparison Using Guideline-based Query of Conventional Radiological Reports and Structured Reports, In Vivo 32(4) (2018) 843-849.
[36] A. Joulin, E. Grave, P. Bojanowski, T. Mikolov, Bag of tricks for efficient text classification, arXiv preprint arXiv:1607.01759 (2016).
[37] L. Breiman, Random forests, Machine learning 45(1) (2001) 5-32.
[38] H. Zou, T. Hastie, Regression shrinkage and selection via the elastic net, with applications to microarrays, JR Stat Soc Ser B 67 (2003) 301-20.
[39] J. Friedman, T. Hastie, R. Tibshirani, Regularization paths for generalized linear models via coordinate descent, Journal of statistical software 33(1) (2010) 1.
[40] C. Cortes, V. Vapnik, Support-vector networks, Machine learning 20(3) (1995) 273-297.
[41] L. Breiman, J. Friedman, C. Stone, R. Olshen, Classification and regression trees., Chapman and Hall/CRC press, 1984.
[42] T. Chen, T. He, Xgboost: extreme gradient boosting, R package version 0.4-2 (2016).
[43] F. Jungmann, S. Kuhn, I. Tsaur, B. Kämpgen, Natural Language Processing in der Radiologie, Der Radiologe 59(9) (2019) 828-832.
[44] M. Wintermark, P.C. Sanelli, G.W. Albers, J. Bello, C. Derdeyn, S.W. Hetts, M.H. Johnson, C. Kidwell, M.H. Lev, D.S. Liebeskind, H. Rowley, P.W. Schaefer, J.L. Sunshine, G. Zaharchuk, C.C. Meltzer, Imaging recommendations for acute stroke and transient ischemic attack patients: A joint statement by the American Society of Neuroradiology, the American College of Radiology, and the Society of NeuroInterventional Surgery, AJNR Am J Neuroradiol 34(11) (2013) E117-27.
[45] D. Deutsche Gesellschaft für Neurologie, Diagnostic of acute cerebrovascular diseases AWMF-030/117 2016. https://www.awmf.org/leitlinien/detail/ll/030-117.html. (Accessed Jan 1, 2020.
[46] V. Cotik, R. Roller, F. Xu, H. Uszkoreit, K. Budde, D. Schmidt, Negation detection in clinical reports written in German, Proceedings of the Fifth Workshop on Building and Evaluating Resources for Biomedical Text Mining (BioTxtM2016), 2016, pp. 115-124.
[47] S. Robertson, H. Zaragoza, The probabilistic relevance framework: BM25 and beyond, Foundations and Trends® in Information Retrieval 3(4) (2009) 333-389.
[48] V.I. Levenshtein, Binary codes capable of correcting deletions, insertions, and reversals, Soviet physics doklady, 1966, pp. 707-710.
[49] P. Kluegl, M. Toepfer, P.-D. Beck, G. Fette, F. Puppe, UIMA Ruta: Rapid development of rule-based information extraction applications, Natural Language Engineering 22(1) (2016) 1-40.
[50] L. Breiman, Classification and regression trees, Routledge2017.
[51] L. Breiman, P. Spector, Submodel Selection and Evaluation in Regression. The X-Random Case, International Statistical Review / Revue Internationale de Statistique 60(3) (1992) 291-319.
[52] T. Hastie, R. Tibshirani, J. Friedman, The elements of statistical learning: Data Mining, Inference and Prediction, 2. ed., Springer, New York, NY2009.
[53] A. Liaw, M. Wiener, Classification and regression by randomForest, R news 2(3) (2002) 18-22.
[54] C. Chen, A. Liaw, L. Breiman, Using random forest to learn imbalanced data, University of California, Berkeley 110 (2004).
[55] C. Strobl, A.-L. Boulesteix, A. Zeileis, T. Hothorn, Bias in random forest variable importance measures: Illustrations, sources and a solution, BMC bioinformatics 8(1) (2007) 1.
[56] T. Parr, K. Turgutlu, C. Csiszar, J. Howard, Beware Default Random Forest Importances, 2018. https://explained.ai/rf-importance/.
[57] A. Paluszynska, P. Biecek, Y. Jiang, randomForestExplainer: Explaining and Visualizing Random Forests in Terms of Variable Importance, version 0.10. 0, R package (2019).
[58] E. Grave, P. Bojanowski, P. Gupta, A. Joulin, T. Mikolov, Learning word vectors for 157 languages, arXiv preprint arXiv:1802.06893 (2018).
[59] M.H. DeGroot, S.E. Fienberg, The comparison and evaluation of forecasters, The statistician (1983) 12-22.
[60] D. Nee, Calibrating classifier probabilities Website, Blog., 2014.
[61] A. Niculescu-Mizil, R. Caruana, Predicting good probabilities with supervised learning, Proceedings of the 22nd international conference on Machine learning, ACM, Bonn, Germany, 2005, pp. 625-632.
[62] M. Kohli, T. Alkasab, K. Wang, M.E. Heilbrun, A.E. Flanders, K. Dreyer, C.E. Kahn, Jr., Bending the Artificial Intelligence Curve for Radiology: Informatics Tools From ACR and RSNA, J Am Coll Radiol 16(10) (2019) 1464-1470.
[63] R.C. Carlos, C.E. Kahn, S. Halabi, Data Science: Big Data, Machine Learning, and Artificial Intelligence, Journal of the American College of Radiology 15(3, Part B) (2018) 497-498.
[64] T. Syeda-Mahmood, Role of Big Data and Machine Learning in Diagnostic Decision Support in Radiology, Journal of the American College of Radiology 15(3, Part B) (2018) 569-576.
[65] Y. Hong, J. Zhang, M.E. Heilbrun, C.E. Kahn, Jr., Analysis of RadLex coverage and term co-occurrence in radiology reporting templates, J Digit Imaging 25(1) (2012) 56-62.

[66] C.E. Kahn, Jr., M.E. Heilbrun, K.E. Applegate, From guidelines to practice: how reporting templates promote the use of radiology practice guidelines, J Am Coll Radiol 10(4) (2013) 268-73.
[67] T.A. Morgan, M.E. Helibrun, C.E. Kahn, Jr., Reporting initiative of the Radiological Society of North America: progress and new directions, Radiology 273(3) (2014) 642-5.
[68] D.L. Weiss, C.P. Langlotz, Structured reporting: patient care enhancement or productivity nightmare?, Radiology 249(3) (2008) 739-47.
[69] S. Hassanpour, C.P. Langlotz, Information extraction from multi-institutional radiology reports, Artificial intelligence in medicine 66 (2016) 29-39.
[70] M. Yetisgen-Yildiz, M.L. Gunn, F. Xia, T.H. Payne, A text processing pipeline to extract recommendations from radiology reports, Journal of Biomedical Informatics 46(2) (2013) 354-362.
[71] D. Zinovev, D. Raicu, J. Furst, S.G. Armato III, Predicting radiological panel opinions using a panel of machine learning classifiers, Algorithms 2(4) (2009) 1473-1502.
[72] I. Banerjee, S. Bozkurt, E. Alkim, H. Sagreiya, A.W. Kurian, D.L. Rubin, Automatic inference of BI-RADS final assessment categories from narrative mammography report findings, Journal of Biomedical Informatics 92 (2019) 103137.
[73] T. Mikolov, I. Sutskever, K. Chen, G.S. Corrado, J. Dean, Distributed representations of words and phrases and their compositionality, Advances in neural information processing systems, 2013, pp. 3111-3119.
[74] I. Banerjee, M.C. Chen, M.P. Lungren, D.L. Rubin, Radiology report annotation using intelligent word embeddings: Applied to multi-institutional chest CT cohort, Journal of Biomedical Informatics 77 (2018) 11-20.
[75] I. Banerjee, S. Madhavan, R.E. Goldman, D.L. Rubin, Intelligent word Embeddings of free-text radiology reports, AMIA Annual Symposium Proceedings, American Medical Informatics Association, 2017, p. 411.
[76] I. Banerjee, S. Madhavan, R.E. Goldman, D.L. Rubin, Intelligent word Embeddings of free-text radiology reports, AMIA Annual Symposium Proceedings, American Medical Informatics Association, 2017, p. 411.
[77] D.L. Rubin, Creating and curating a terminology for radiology: ontology modeling and analysis, J Digit Imaging 21(4) (2008) 355-62.
[78] K.C. Wang, Standard Lexicons, Coding Systems and Ontologies for Interoperability and Semantic Computation in Imaging, J Digit Imaging 31(3) (2018) 353-360.
[79] R.W. Filice, C.E. Kahn, Integrating an Ontology of Radiology Differential Diagnosis with ICD-10-CM, RadLex, and SNOMED CT, Journal of Digital Imaging 32(2) (2019) 206-210.
[80] E. Pons, L.M.M. Braun, M.G.M. Hunink, J.A. Kors, Natural language processing in radiology: a systematic review, Radiology 279(2) (2016) 329-343.
[81] T. Hastie, R. Tibshirani, J. Friedman, High-Dimensional Problems: p N, The Elements of Statistical Learning: Data Mining, Inference, and Prediction, Springer New York, New York, NY, 2009, pp. 649-698.
[82] W.K. Tan, S. Hassanpour, P.J. Heagerty, S.D. Rundell, P. Suri, H.T. Huhdanpaa, K. James, D.S. Carrell, C.P. Langlotz, N.L. Organ, E.N. Meier, K.J. Sherman, D.F. Kallmes, P.H. Luetmer, B. Griffith, D.R. Nerenz, J.G. Jarvik, Comparison of Natural Language Processing Rules-based and Machine-learning Systems to Identify Lumbar Spine Imaging Findings Related to Low Back Pain, Academic radiology 25(11) (2018) 1422-1432.
[83] J. Li, D. Jurafsky, Do multi-sense embeddings improve natural language understanding?, arXiv preprint arXiv:1506.01070 (Computation and Language (cs.CL)) (2015).
[84] P. Richter-Pechanski, A. Amr, H.A. Katus, C. Dieterich, Deep Learning Approaches Outperform Conventional Strategies in De-Identification of German Medical Reports, Studies in health technology and informatics 267 (2019) 101-109.
[85] J. Howard, S. Ruder, Universal language model fine-tuning for text classification, arXiv preprint arXiv:1801.06146 (2018).
[86] D. Capper, D.T.W. Jones, M. Sill, V. Hovestadt, D. Schrimpf, D. Sturm, C. Koelsche, F. Sahm, L. Chavez, D.E. Reuss, A. Kratz, A.K. Wefers, K. Huang, K.W. Pajtler, L. Schweizer, D. Stichel, A. Olar, N.W. Engel, K. Lindenberg, P.N. Harter, A.K. Braczynski, K.H. Plate, H. Dohmen, B.K. Garvalov, R. Coras, l. H\"o, Annett, E. Hewer, M. Bewerunge-Hudler, M. Schick, R. Fischer, R. Beschorner, J. Schittenhelm, O. Staszewski, K. Wani, P. Varlet, M. Pages, P. Temming, D. Lohmann, F. Selt, H. Witt, T. Milde, O. Witt, E. Aronica, F. Giangaspero, E. Rushing, W. Scheurlen, C. Geisenberger, F.J. Rodriguez, A. Becker, M. Preusser, C. Haberler, R. Bjerkvig, J. Cryan, M. Farrell, M. Deckert, J.u. Hench, rgen, S. Frank, J. Serrano, K. Kannan, A. Tsirigos, c. Br\"u, Wolfgang, S. Hofer, S. Brehmer, M. Seiz-Rosenhagen, n. H\"a, Daniel, V. Hans, S. Rozsnoki, J.R. Hansford, P. Kohlhof, B.W. Kristensen, M. Lechner, B. Lopes, C. Mawrin, R. Ketter, A. Kulozik, Z. Khatib, F. Heppner, A. Koch, A. Jouvet, C. Keohane, h. M\"u, Helmut, W. Mueller, U. Pohl, M. Prinz, A. Benner, M. Zapatka, N.G. Gottardo, P.H.a. Driever, iz, C.M. Kramm, l. M\"u, Hermann L., S. Rutkowski, K. von Hoff, h. Fr\"u, Michael C., A. Gnekow, G. Fleischhack, S. Tippelt, G. Calaminus, C.-M. Monoranu, A. Perry, C. Jones, T.S. Jacques, B. Radlwimmer, M. Gessi, T. Pietsch, J. Schramm, G. Schackert, M. Westphal, G. Reifenberger, P. Wesseling, M. Weller, V.P. Collins, m. Bl\"u, Ingmar, M. Bendszus, J.u. Debus, rgen, A. Huang, N. Jabado, P.A. Northcott, W. Paulus, A. Gajjar, G.W. Robinson, M.D. Taylor, Z. Jaunmuktane, M. Ryzhova, M. Platten, A. Unterberg, W. Wick, M.A. Karajannis, M. Mittelbronn, T. Acker, C. Hartmann, K. Aldape, l. Sch\"u, Ulrich, R. Buslei, P. Lichter, M. Kool, C. Herold-Mende, D.W. Ellison, M. Hasselblatt, M. Snuderl, S. Brandner, A. Korshunov, A. von Deimling, S.M. Pfister, DNA methylation-based classification of central nervous system tumours, Nature 555 (2018) 469.
[87] N.V. Chawla, K.W. Bowyer, L.O. Hall, W.P. Kegelmeyer, SMOTE: synthetic minority over-sampling technique, Journal of artificial intelligence research 16 (2002) 321-357.

 doi:10.20944/preprints202004.0354.v1

Figures

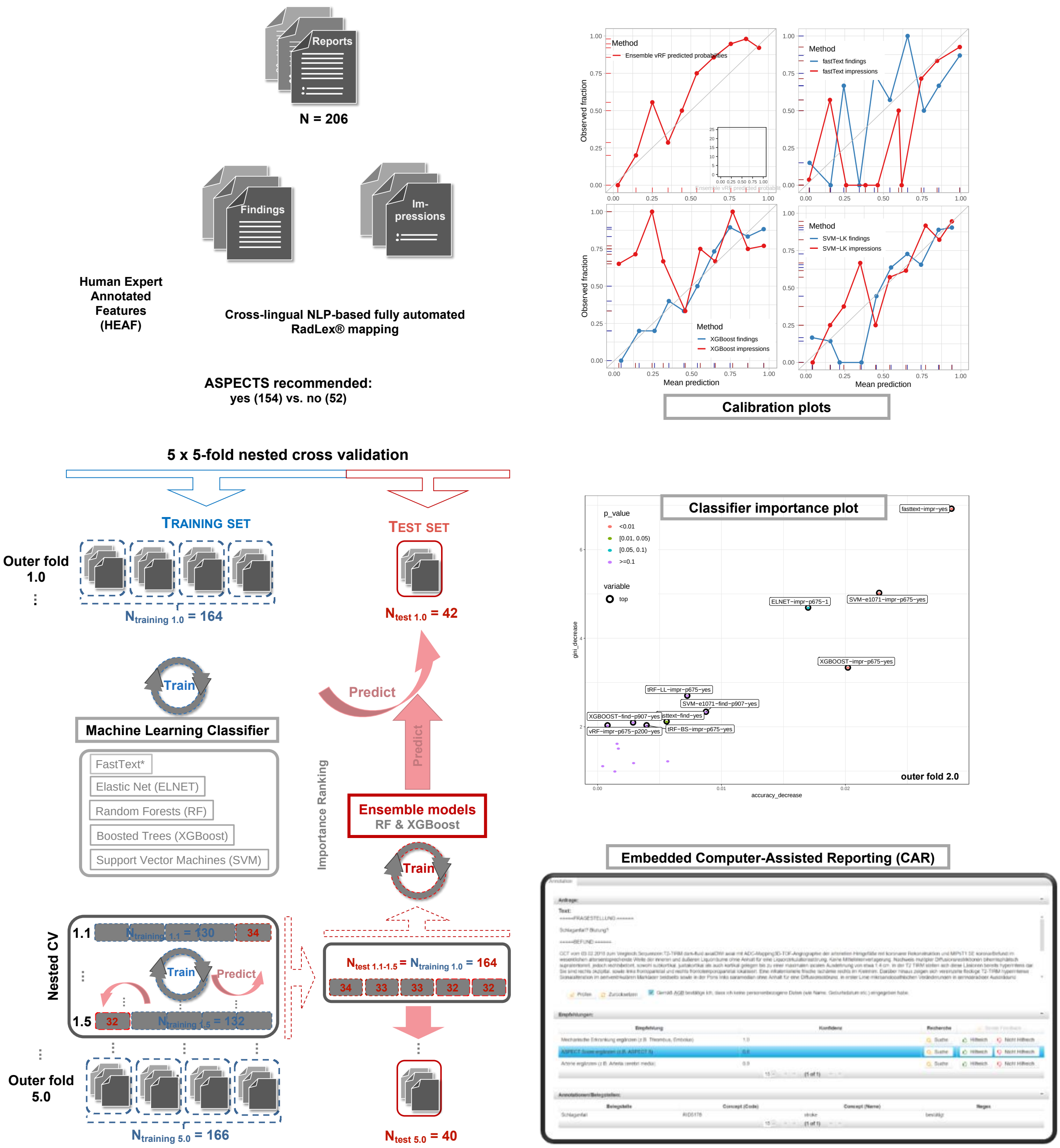

Graphical abstract

Preprints (www.preprints.org) | NOT PEER-REVIEWED | Posted: 19 April 2020 doi:10.20944/preprints202004.0354.v1

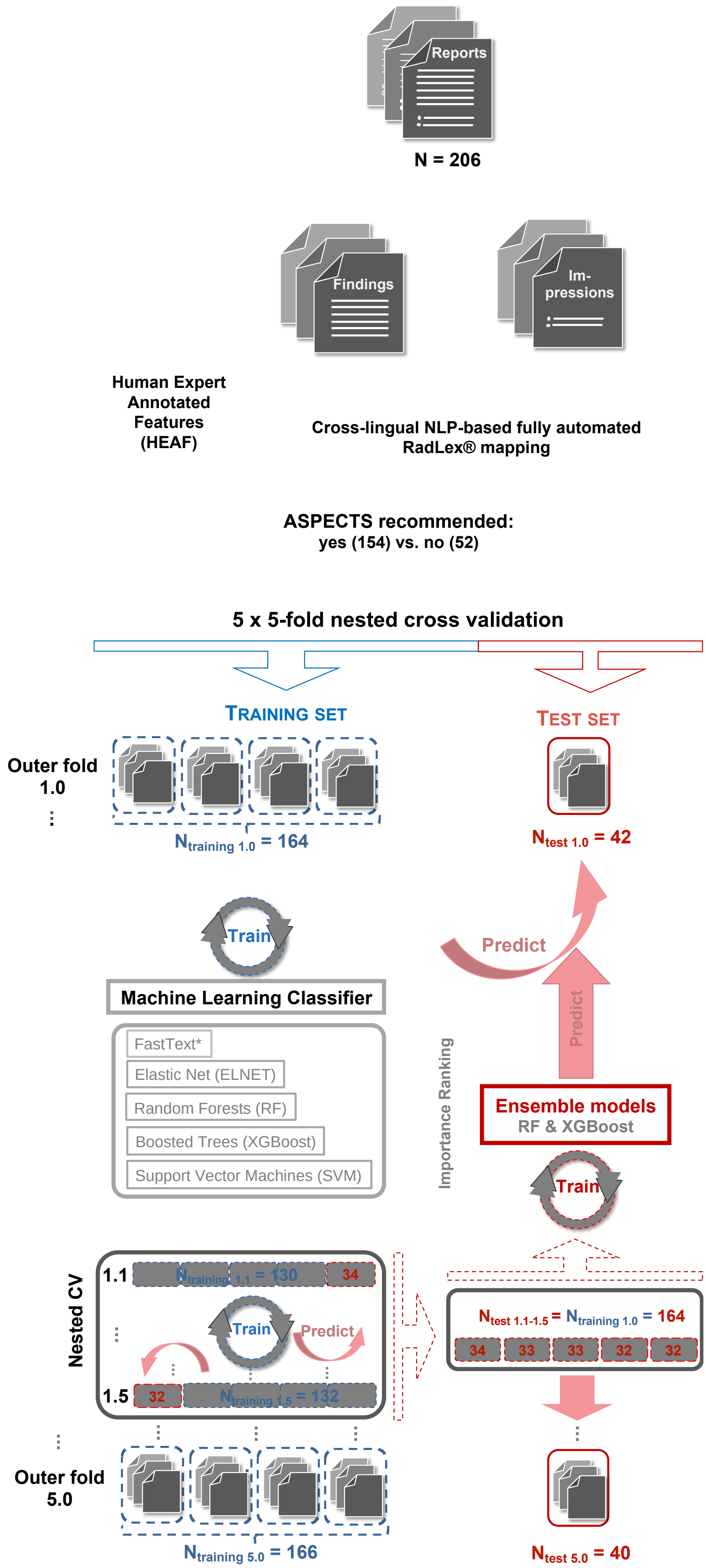

Preprints (www.preprints.org) | NOT PEER-REVIEWED | Posted: 19 April 2020 doi:10.20944/preprints202004.0354.v1

Figure 1 shows the 5 x 5-fold nested cross validation setup, which was used to evaluate all machine learning (ML) algorithms and to train the second layer model as a meta/ensemble-learner on top of the combined predictions of these base ML classifiers. Human experts had access to both the findings and impression sections as well as the clinical question field of the reports to generate target labels ASPECTS recommended "yes" (n=154) vs. "no" (n=52) and to extract clinico-radiologically relevant features (HEAF). The findings and the impressions were each passed through a fully automated cross-lingual (German-English) natural language processing (NLP) pipeline to generating RadLex® mappings. The pipeline can be accessed at mmatt.shinyapps.io/rasp. In order to prevent information leakage, the second layer meta/ensemble models (random forests [RF] and boosted trees [XGBoost]) were trained on the combined inner fold test (i.e. sum of nested validation $\Sigma N_{test\_1.1-1.5}$) sets. These second layer models were used to derive objective importance rankings of the individual ML-classifiers. To ensure direct comparability between the investigated ML-algorithms, the data partitioning was identical (i.e. each model was trained and fitted on the very same subsamples of the data). However, fastText was fitted directly on German report texts, whereas other ML-algorithms were fitted on both HEAF and NLP-based RadLex® mappings. The final performance measure of the classifiers was calculated as the 5-fold cross-validated average on the outer folds (see Tables 1, 2 and 3).

Preprints (www.preprints.org) | NOT PEER-REVIEWED | Posted: 19 April 2020 doi:10.20944/preprints202004.0354.v1

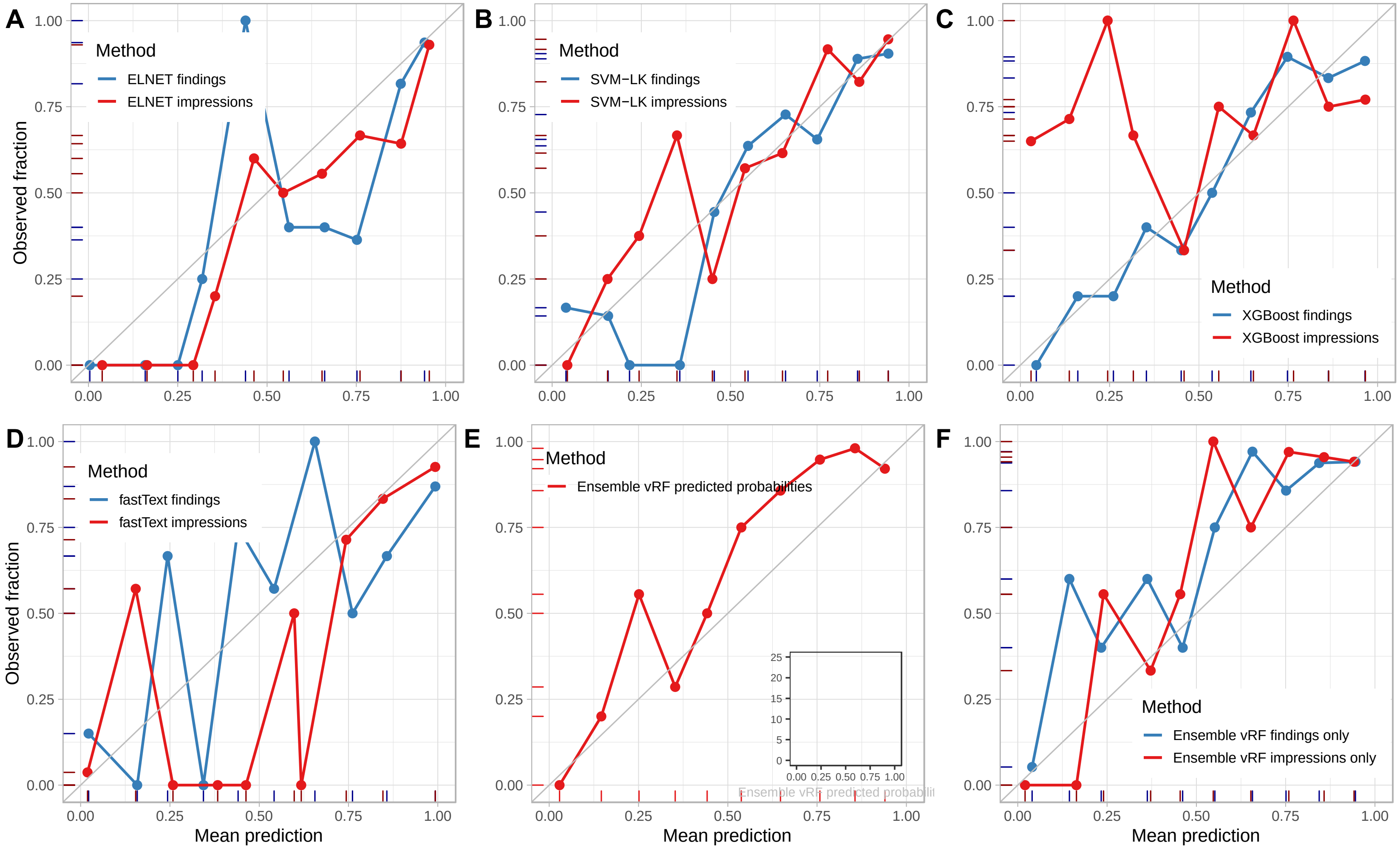

Figure 2 depicts the visual calibration profiles (reliability plots) of the most important machine learning classifiers based on the random forests ensemble when fitting the automated RadLex® mappings (all outer folds combined, N=206). Points represent the mean predictions and corresponding

observed fractions of respective “ASPECTS recommended: yes” cases for each ten bins (i.e. 0-0.1, …, 0.9-1.0) of the probability domain. The rug plots at the top (red; impressions) and bottom (blue; findings) visualize the distribution of the probability estimates of the respective ML-algorithm. Each line indicates an estimate of a single case (N=206). ELNET (**A**) was more suitable for the impressions (red) particularly in the 0.50-0.75 range, corresponding to its top 3 ranked accuracy. Linear kernel SVMs (**B**) showed well-calibrated estimates for the 0.50-1.0 probability domain for both the findings (blue) and the impressions (red). XGBoost (**C**) showed the best overall calibration profile among all investigated ML-models. It presented an almost perfect calibration curve (grey diagonal line) on the findings for the whole probability domain (0-1) while being the most accurate ML-classifier (Table 2). Although fastText (**D**) showed remarkable accuracies (highest overall) when fitting the impressions (red curve) and the third best on the findings (blue curve), its probability estimates were poorly calibrated – particularly on the findings and for “ASPECTS recommended: no” cases (see Table 2). The RF ensemble (**E**) showed a reasonably well-calibrated profile when trained on the probability estimates of all ML-algorithms (16x ML-models) including both of which were generated on the findings and impressions sections (see Table 3). The inset of the histogram shows the bimodal distribution of the probability estimates for the “ASPECTS recommended: yes” label of the RF ensemble. For the most part, the ensemble was “quite sure” about the label (maximum in the range of 0.75-1.0). Also, it showed (**F**) similar calibration profiles when trained either only on ML-model estimates of the findings (blue; 8x models) or the impressions (red; 8x models).

Preprints (www.preprints.org) | NOT PEER-REVIEWED | Posted: 19 April 2020 doi:10.20944/preprints202004.0354.v1

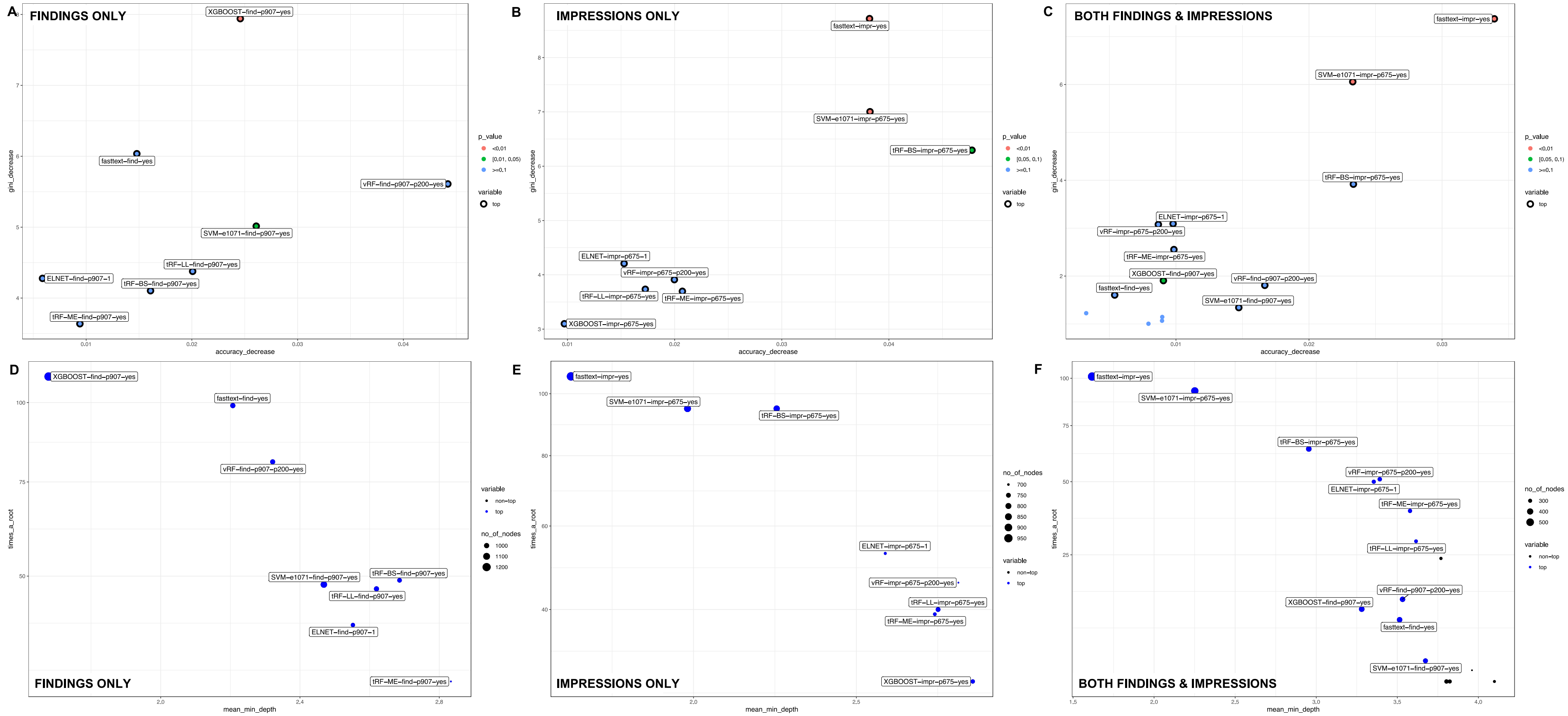

Figure 3 shows the multi-way importance plots of the investigated machine learning algorithms based on the random forests ensemble when fitting the automated RadLex® mappings of the first outer fold test set ($N_{test.1.0}$=42). Subplots **A, B** and **C** show the importance measures (y-axis: mean decrease in Gini index; x-axis: mean decrease in accuracy) that are based on the role a ML-algorithm plays in the prediction of the RF ensemble. Notably, the mean decrease in accuracy (x-axis) is a more robust measure for variable importance[6, 53, 55, 56]. P-values are based on a binomial

Preprints (www.preprints.org) | NOT PEER-REVIEWED | Posted: 19 April 2020 doi:10.20944/preprints202004.0354.v1

distribution of the number of nodes split on the variable. Subplots **D**, **E** and **F** focus on three importance measures that are derived from the structure of the trees in the forest including i) mean_min_depth (x-axis) of the first split on the variable; ii) number of trees in which the root is split on the variable ("variable": blue patch non-top or top); iii) the total number of nodes in the forest that split on that ML-classifier (no_of_nodes). Subplots **A** and **D**; **B** and **E**; and **C** and **F** are the corresponding plots to each other when fitting ML-models of the findings only, impressions only and both, respectively. When combining ML-classifiers trained on the findings sections only (**A**), XGBoost ($p<0.01$) and linear kernel SVMs ($p<0.05$) were the only two significant predictors. Likewise, for the impressions (**B**), fastText ($p<0.01$) was by far the most important predictor. Nonetheless, SVM-LK ($p<0.01$) and brier score-tuned RF (tRF-BS) were also significant ($p<0.05$). When we combined all ML-models (findings & impressions; **C**), fastText ($p<0.01$) and SVM-LK ($p<0.01$) based on the impressions dominated the importance rankings, however, (although less relevant) XGBoost estimates using the findings sections stayed also significant ($p<0.05$).

 doi:10.20944/preprints202004.0354.v1

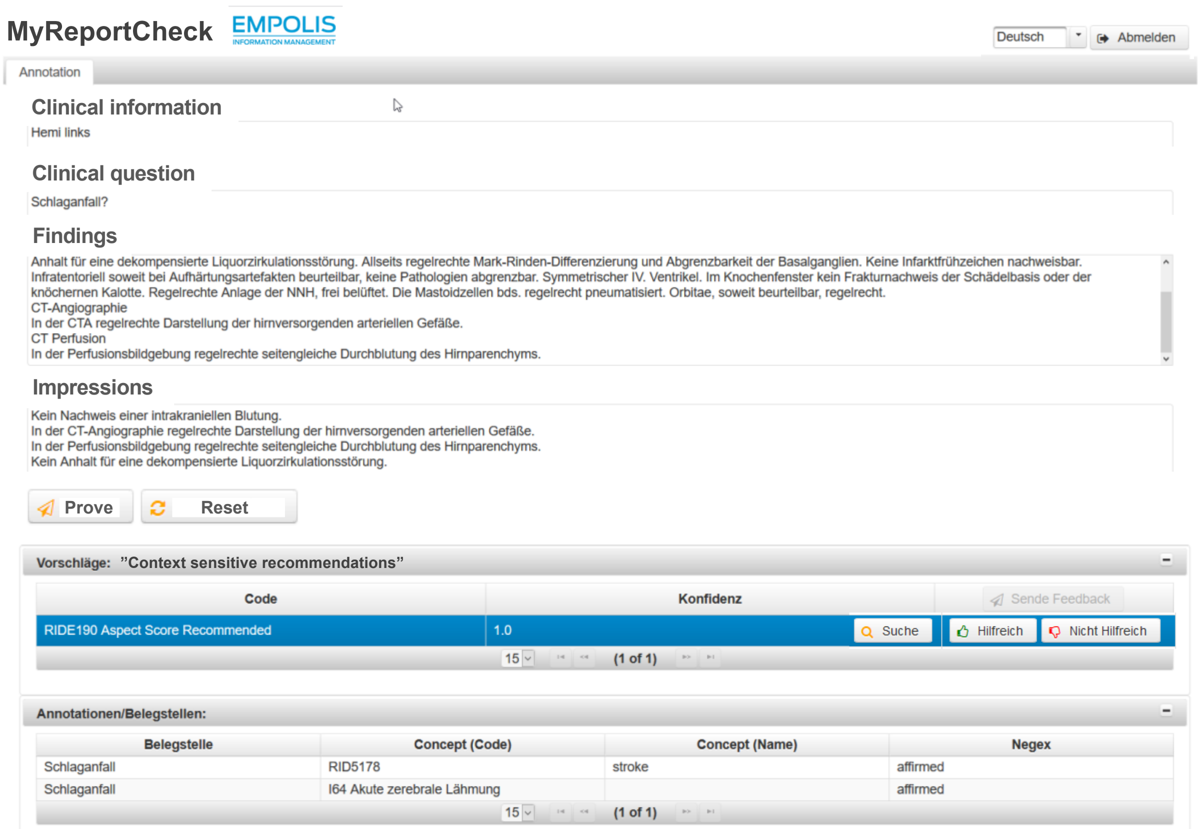

Figure 4 depicts the prototype graphical user interface of our context-sensitive CAR tool "MyReportCheck", which utilizes our embedded machine learning framework on fully automated RadLex® mappings for recommending ASPECTS during the reporting of neuroradiological emergencies. The software solution is available as service from Empolis Information Management GmbH (Kaiserslautern, Germany).